PNL-10746
UC-510

EVALUATION OF THE SINGLE-PASS FLOW-THROUGH TEST TO SUPPORT A LOW-ACTIVITY WASTE SPECIFICATION

B. P. McGrail
D. K. Peeler[a]

September 1995

Prepared for
the U.S. Department of Energy
under Contract DE-AC06-76RLO 1830

Pacific Northwest Laboratory
Richland, Washington 99352

[a] Westinghouse Savannah River Company
Aiken, South Carolina 29808

DISCLAIMER

Portions of this document may be illegible in electronic image products. Images are produced from the best available original document.

SUMMARY

A series of single-pass flow-through (SPFT) tests was performed on five reference low-activity waste glasses and a reference glass from the National Institute of Standards and Technology to support a product specification for low-activity waste (LAW) forms. The results showed that the SPFT test provides a means to quantitatively distinguish among LAW glass forms in terms of their forward reaction rate at a given temperature and solution pH.

Two of the test glasses were also subjected to SPFT testing at Argonne National Laboratory (ANL). Forward reaction rate constants calculated from the ANL test data were 100 to over 1000 times larger than the values obtained from the SPFT tests conducted at PNL. An analysis of the ANL results showed that they were inconsistent with independent measurements done on glasses of similar composition, the known pH-dependence of the forward rate, and with the results from low surface-area-to-volume, short duration product consistency tests. Because the data set obtained from the SPFT tests done at PNL was consistent with each of these same factors, a detailed examination of the test procedures used at both laboratories was performed to determine the cause(s) of the discrepancy. The omission of background subtraction in the data analysis procedure and the short-duration (on the order of hours) of the ANL tests are factors that may have significantly affected the calculated rates.

CONTENTS

LIST OF FIGURES

LIST OF TABLES

INTRODUCTION

This report presents the results of a testing program conducted at Pacific Northwest Laboratory (PNL)[1] to provide information needed to support a product specification for low-activity waste (LAW) forms. A key component of the product specification will be a radionuclide release requirement that (1) identifies a measurable characteristic of the product that bounds the long-term radionuclide release rate in the disposal environment, (2) specifies an acceptance criterion, and (3) identifies a testing method that is suitable for assessing compliance with the acceptance criterion. Initial performance assessment calculations indicate the maximum acceptable long-term release rate of ^{99}Tc from the disposal site is about 2.4×10^{-2} Ci/a, which is equivalent to a glass corrosion rate of 10^{-3} g/m^2·d. However, this estimate is based on many unsubtantiated assumptions regarding water recharge rate, radionuclide inventories, and waste form dimensions. It also neglects the effects of other engineered or natural barriers.

Though a waste form will not be specified in the LAW product specification, an approach for bounding radionuclide release rates from a silicate glass waste form will be presented. The tests described in this report were conducted to determine whether the single-pass flow-through (SPFT) method is suitable for providing these bounding estimates. Addtional testing was conducted at Argonne National Laboratory (ANL) to evaluate the product consistency test (PCT) for the same purpose. The PCT is commonly used to compare the consistency of various glass waste forms, and has been standardized by the ASTM (ASTM 1994). The PCT procedure was modified in the tests run at ANL to maintain more dilute solutions that were thought to more closely approximate conditions in the SPFT test. A limited set of SPFT tests were also conducted at ANL, although the test method and data evaluation procedures used at ANL were substantially different than those used in this report. Complete information on the testing and results obtained at ANL is available (Ebert et al. 1995).[2]

[1]Pacific Northwest Laboratory is operated for the U.S. Department of Energy by Battelle Memorial Institute under Contract DE-AC06-76RLO 1830.

[2]Ebert, W. L., A. J. Bakel, S. F. Wolf, and J. K. Bates. 1995. *ANL Testing Program to Support the Low-Level Product Durability Specification.* Unpublished letter report.

BACKGROUND

The most desirable test for a LAW product release requirement would be a test that is run for a short time, is sensitive to variations in the composition of the product, and provides results that could be directly correlated to long-term radionuclide release rates in the disposal system. Unfortunately, such a test does not exist. Over 20 years of experimental and theoretical research on silicate glass/water interactions has shown that an extraordinary amount of information is required before such calculations can be attempted for just the reaction of the glass and water alone (Bates et al. 1994). Evaluations of radionuclide release rates from the disposal system requires computation of the time and spatial variation in the physical and chemical environment of the site that can only be done with sophisticated multicomponent, reactive transport computer codes (McGrail and Mahoney 1995). Clearly, such modeling is beyond the scope of a LAW product compliance specification.

One valid means of circumventing the difficulty of determining long-term release rates from a waste form is by applying bounding principles to the problem. By applying bounding principles, it is usually possible to simplify the analysis and provide results that are relatively easy to understand and defend. The idea of bounding radionuclide release estimates from high-level waste packages has been endorsed by the National Academy of Sciences in their Waste Isolation System study (Pigford et al. 1983).

Fortunately, it is relatively easy to bound radionuclide release rates from a silicate glass waste form using an experimental method that is commonly used for measuring reaction rates of minerals (Knauss and Wolery 1986) and glasses (Knauss et al. 1990; McGrail and Olson 1992). The SPFT test is designed to measure reaction rates under tightly-controlled, dilute solution conditions. Dissolution of silicate glasses and minerals in an aqueous solution is a dissociation-association process in which two or more soluble species are released into or removed from solution. It is subject to the common ion effect, which occurs when a solution already contains the same ions that would be released when a solid dissolves (or precipitates). The presence of common ions released from the glass or from other sources reduces the net rate of release relative to the rate in pure water. Hence, the idea of the SPFT test is to remove the elements released into

solution from glass dissolution by continuously introducing fresh water into the system. Run properly, the SPFT test provides a direct measure of the so-called "forward reaction rate." The forward reaction rate is the maximum rate at which a silicate glass or mineral can dissolve at a given temperature and pH. Once the forward rate is known, it is simple to calculate the absolute upper bound on the release rate of any glass component, including a radionuclide such as ^{99}Tc.

Using the SPFT test as a LAW product acceptance test is attractive for a number of reasons. First, the test provides a direct measure of the maximum possible corrosion rate of a glass that can be used in performance assessment analyses. Second, the test eliminates the ambiguity that is unavoidable in interpreting the results from a closed-system test such as the PCT. In the PCT, the solution pH and concentration of glass components change as a function of time. The changing pH is particularly problematic because SPFT tests show that the forward reaction rate increases by approximately a factor of 3 for every unit increase in pH over the pH range from 7 to 12. Also, secondary phases can form in the PCT, which means that the solution concentration of some components may not give an accurate measure of the glass corrosion rate. Finally, because the PCT is a closed-system test, the results, particularly at early times and/or temperatures <40°C, are subject to phenomena such as ion-exchange, dissolution of fines, and reaction of highly strained fracture surfaces that are not true measures of the glass dissolution rate.

The major difficulty to be overcome with the SPFT test is that compared with the PCT, the experiment is considerably more complicated to run. Also, when using samples with unknown corrosion rates, it is usually necessary to run several scoping tests to determine the flow rate that is required to maintain the desired dilute conditions, yet give solution concentration values that are significantly above the background concentration of an important element, like Si. Although the SPFT test is a commonly used technique in kinetics studies of rock-water reactions, compared with the PCT, the method has seen relatively little use in the waste management community. Consequently there is no standardized test method available. The method used in this study is similar to the technique described by Knauss and Wolery (1986). Both our method and the method used by Knauss and Wolery are very different from the technique used at ANL. Ebert et al. (1995) classify their method as "high-flow rate" and our method as "low-flow" rate. Although this classification accurately describes the different flow rates used, we believe the

subjective nature of the term "low-flow" versus "high-flow" is not particularly useful. As long as the experimentalist can show that the test conditions maintain dilute solution conditions such that precipitation of major secondary phases is prevented, then the distinction of high-flow versus low-flow is unimportant and the tests should give identical results, provided the data are interpreted in the same manner.

EXPERIMENTAL

A description of the experimental methods and materials used is given in the following sections.

MATERIALS

Six glasses were evaluated in this study. The composition of these glasses is given in Table 1. The tests were conducted at 40, 70, and 90°C using two different solutions to adjust the solution pH. The solution composition and the computed pH at temperature are shown in Table 2. The glass samples were prepared according to standard PCT methods and the -100+200 mesh size fraction was used for all tests. Glass density was measured for each glass and is reported in Table 3. The glass density was used to compute the change in surface area that occurs over the course of the test. The procedure used for this calculation is given in Appendix A.

Table 1. Composition of Test Glasses in Oxide Mass Fraction

Glass ID	Al_2O_3	B_2O_3	CaO	K_2O	MgO	Na_2O	P_2O_5	SiO_2	ZrO_2	Others
LD4-9012	0.1200	0.0900	-	0.0146	3.0E-05	0.2000	0.0019	0.5591	-	0.0144
LD6-5412	0.1200	0.0500	0.0400	0.0146	3.0E-05	0.2000	0.0019	0.5591	-	0.0144
L7-15	0.1245	0.0539	0.0431	0.0024	-	0.1500	0.0089	0.6119	-	0.0053
L7-25	0.1155	0.0461	0.0369	0.0041	-	0.2500	0.0148	0.5238	-	0.0088
SRM622	0.0180	-	0.1150	0.0004	0.0050	0.1400	-	0.7170	-	0.0046
L8-3	0.0900	0.0500	0.0400	0.0033	-	0.2000	0.0119	0.5678	0.0300	0.0070

Table 2. Composition of Buffer Solutions Used for Single-Pass Flow-Through Tests. Solution pH and ionic strength values were calculated with the EQ3NR Code.

Buffer	Composition	I	pH 20°C	pH 40°C	pH 70°C	pH 90°C
1	0.005 m H_3BO_3 + 0.0020 m LiOH	0.0019	9.09	8.91	8.70	8.59
2	0.005 m LiCl + 0.0107 m LiOH	0.0153	12.14	11.50	10.78	10.39

Table 3. Measured Density of Test Glasses

Glass ID	Density, g/cm^3
LD4-9012	2.48
LD6-5412	2.57
L7-15	2.47
L7-25	2.52
L8-3	2.57
SRM622	2.51

TEST METHOD

All the SPFT tests were conducted in accordance with "GDL-FTP: Single-Pass Flow-Through Test Procedure, Rev. 0." A schematic of the single-pass flow-through apparatus used for all the tests discussed in this report is given in Figure 1. Although the schematic illustrates only a single cell, our apparatus has a capacity of 24 individual cells and 13 different pH buffers that can be run simultaneously. The apparatus features an indirect flow path, i.e., the aqueous solution is not pumped directly through the sample. This design has two key advantages: 1) bubbles that form in the fluid transfer lines cannot become entrained in the porous glass bed and thus potentially affect the exposed sample surface area, and 2) a gas or gas mixture can continuously flow through the cell. This allows the experimentalist to examine the effects of changing the partial pressure of a gas on the reaction kinetics. Fluid is pumped from the buffer solution reservoir into a tri-port staging vessel where it is transferred periodically by gas pressure. The periodic fluid transfer occurs because fluid will rise in the tri-port vessels until the solution and the fluid line come into contact, closing the gas flow path. Pressure then builds up in the tri-port vessel, which initiates the fluid transfer into the reaction cell in the oven. Fluid will continue to transfer, and thus reduce the height of the solution in the tri-port vessel, until surface tension between the outlet tube and the fluid is overcome. At that point, contact between the outlet tube and the fluid in the tri-port vessel is broken, fluid transfer halts, and gas flow resumes through both the tri-port vessel and the reaction cell.

Although periodic solution replenishment is a common batch experimental technique (such as in the ANS 16.1 test), the practice severely complicates the interpretation of the test results because of the periodic and abrupt change in the solution chemistry that occurs after a replenish-

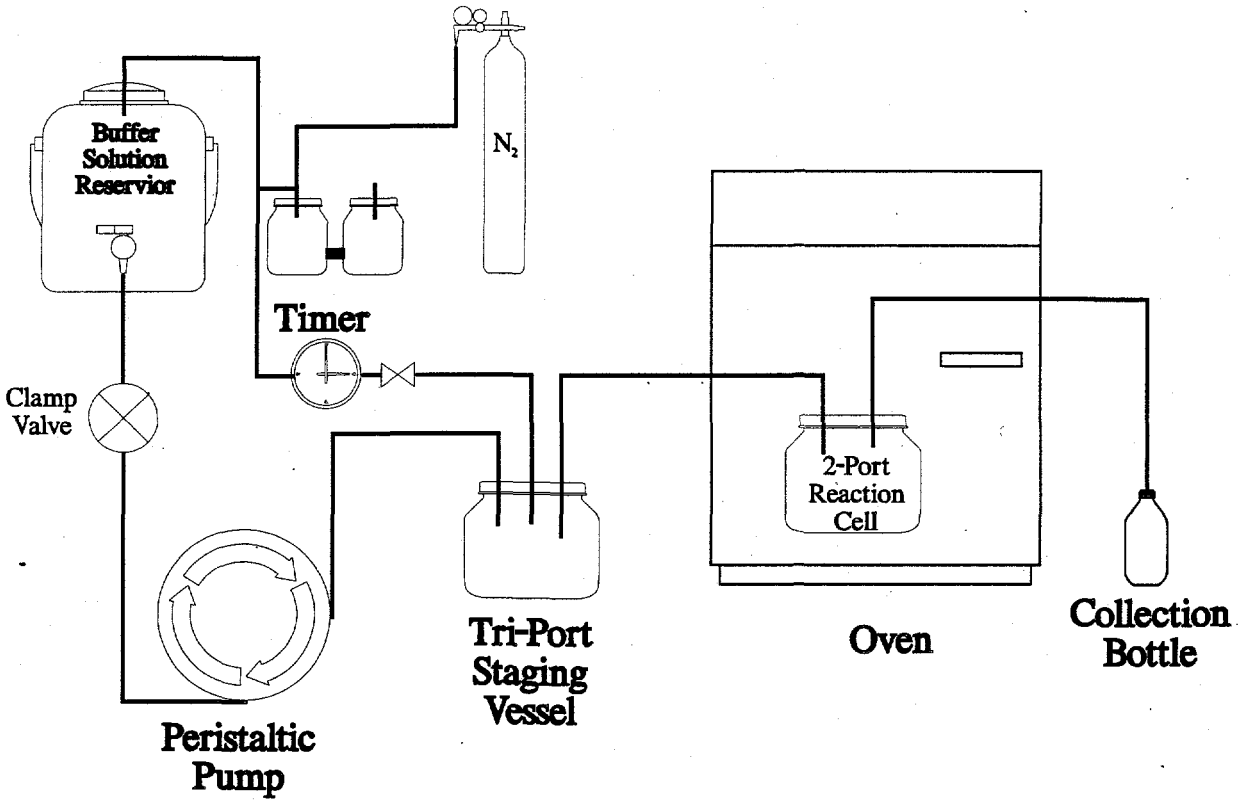

Figure 1. Schematic of Single-Pass Flow-Through Apparatus

ment is done. In the SPFT, however, the solution transfer occurs automatically many times each day (depending on the flow rate), and because the solution always remains dilute, the small variation in the solution concentrations that occurs between pulses cannot affect the test results.

Effluent from each cell is collected in a bottle that is sampled at selected intervals. At each sample interval, the solution pH is measured, and a sample from each collection bottle is taken and acidified with 1 vol% of Ultrex nitric acid. The acidified samples were then analyzed by ICP-AES. No pH variations were detectable in any of the tests from the nominal pH values of the starting buffer solutions. Flow rate is determined from gravimetric analysis of the fluid collected in each collection bottle between samplings. Flow rate variations are less than 5% based upon past experience from the over 500 tests that have been run to date.

TEST MATRIX

The matrix of SPFT tests that were run is given in Table 4. The test temperature can be identified by the 40, 70, or 90 enumeration in the Test ID. Not shown in Table 4 are the blank tests that are run with each test. The blank cells are treated in exactly the same manner as the cells with glass samples.

Table 4. Matrix of SPFT Tests

Test ID	Cell	Glass ID	Buffer Type	Mass
PRIV95-40-1	1	LD6-5412	0.005m H_3BO_3 + 0.0020m LiOH	0.9944
PRIV95-40-1	2	LD4-9012	0.005m H_3BO_3 + 0.0020m LiOH	0.9953
PRIV95-40-1	3	L7-15	0.005m H_3BO_3 + 0.0020m LiOH	1.0040
PRIV95-40-1	4	L7-25	0.005m H_3BO_3 + 0.0020m LiOH	0.9981
PRIV95-40-1	5	L8-3	0.005m H_3BO_3 + 0.0020m LiOH	0.9970
PRIV95-40-1	6	SRM622	0.005m H_3BO_3 + 0.0020m LiOH	0.9988
PRIV95-40-1	13	LD6-5412	0.005m LiCl + 0.0107m LiOH	0.9956
PRIV95-40-1	14	LD4-9012	0.005m LiCl + 0.0107m LiOH	0.9880
PRIV95-40-1	15	L7-15	0.005m LiCl + 0.0107m LiOH	0.9882
PRIV95-40-1	16	L7-25	0.005m LiCl + 0.0107m LiOH	0.9939
PRIV95-40-1	17	L8-3	0.005m LiCl + 0.0107m LiOH	0.9943
PRIV95-40-1	22	SRM622	0.005m LiCl + 0.0107m LiOH	0.9786
PRIV95-70-1	1	LD6-5412	0.005m H_3BO_3 + 0.0020m LiOH	0.9845
PRIV95-70-1	2	LD4-9012	0.005m H_3BO_3 + 0.0020m LiOH	0.9830
PRIV95-70-1	3	L7-15	0.005m H_3BO_3 + 0.0020m LiOH	0.9955
PRIV95-70-1	4	L7-25	0.005m H_3BO_3 + 0.0020m LiOH	0.9873
PRIV95-70-1	5	L8-3	0.005m H_3BO_3 + 0.0020m LiOH	0.9980
PRIV95-70-1	6	SRM622	0.005m H_3BO_3 + 0.0020m LiOH	0.9883
PRIV95-70-1	13	LD6-5412	0.005m LiCl + 0.0107m LiOH	0.9971
PRIV95-70-1	14	LD4-9012	0.005m LiCl + 0.0107m LiOH	0.9979
PRIV95-70-1	15	L7-15	0.005m LiCl + 0.0107m LiOH	0.9846
PRIV95-70-1	16	L7-25	0.005m LiCl + 0.0107m LiOH	1.0015
PRIV95-70-1	17	L8-3	0.005m LiCl + 0.0107m LiOH	0.9942
PRIV95-70-1	22	SRM622	0.005m LiCl + 0.0107m LiOH	0.9970
PRIV95-90-1	1	SRM622	0.005m H_3BO_3 + 0.0020m LiOH	0.9957
PRIV95-90-1	4	LD6-5412	0.005m H_3BO_3 + 0.0020m LiOH	1.0003
PRIV95-90-1	14	LD4-9012	0.005m H_3BO_3 + 0.0020m LiOH	0.9832
PRIV95-90-1	15	L7-15	0.005m H_3BO_3 + 0.0020m LiOH	0.9775
PRIV95-90-1	16	L7-25	0.005m H_3BO_3 + 0.0020m LiOH	0.9696
PRIV95-90-1	17	L8-3	0.005m H_3BO_3 + 0.0020m LiOH	0.9737
GDL-95L-90-1	4	L7-15	0.005m LiCl + 0.0107m LiOH	0.9939
GDL-95L-90-1	5	L7-25	0.005m LiCl + 0.0107m LiOH	0.9888
GDL-95L-90-1	19	L8-3	0.005m LiCl + 0.0107m LiOH	0.9845
VEN95-90-1	2	LD4-9012	0.005m LiCl + 0.0107m LiOH	1.0273
VEN95-90-1	4	LD6-5412	0.005m LiCl + 0.0107m LiOH	1.0068
VEN95-90-1	8	SRM622	0.005m LiCl + 0.0107m LiOH	1.0123

RESULTS

A detailed listing of the experimental results from the SPFT tests is given in Appendix B. Below, the data analysis methods used to calculate normalized corrosion rates are discussed.

ANALYSIS METHOD

The glass corrosion rate was calculated for each component i and at each time interval j using the following formula

$$R_{i,j} = (C_{i,j} - \overline{C}_{i,b}) \frac{Q_j}{f_i S_j} \tag{1}$$

where Q_j = flow rate at time period j, m^3/d
$C_{i,j}$ = concentration of component i, at time period j
$\overline{C}_{i,b}$ = mean background concentration of component i
f_i = mass fraction of component i
S_j = average total glass surface area over time period j-1 to j, m^2.

A description of the method used to calculate the time-dependent surface area of the glass is given in Appendix A. For the 40°C experiments, the mass loss never exceeded more than 5% so the surface area correction was negligible. However, for the 90°C tests, as much as 22% mass loss was calculated in one test and the surface area correction for these data had a signficant effect on the results. Negative rate values indicate that either the analytical detection limit was used to compute the corrosion rate or the measured concentration was less than the mean background concentration for that element.

All of the corrosion rate calculations presented in this report were done with the aid of computer code designed for the analysis of SPFT data. Figure 2 illustrates a typical screen display. The Single-Pass Flow-Through Analyzer (SIPFT) code executes on any personal computer or workstation capable of running the Microsoft Windows™ operating system. The code operates by querying a database file that contains all of the SPFT test results, glass composition, and glass physical property data. The query then returns a record set that matches the criteria specified by the user. There are also options for displaying the data in raw concentration units, as normalized

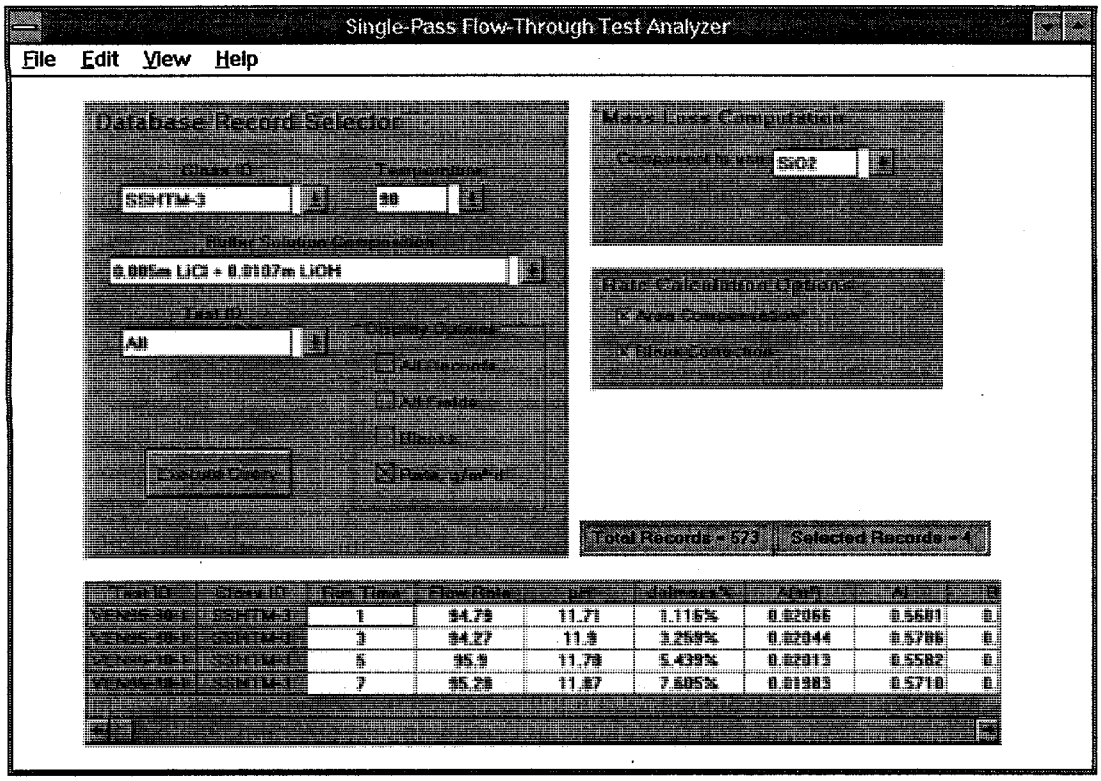

Figure 2. Typical Screen Display from the SIPFT Code

rates, and to disregard background subtraction and surface area changes in computing the normalized rates.

SOLUTION CONCENTRATION RESULTS

Many of the trends in the time-dependence of the solution concentration results were essentially identical among the test glasses. Consequently, only selected examples will be presented here to illustrate the major features. Figure 3 shows the time-dependent change in the solution concentration of each major glass component as a function of time for glass LD4-9012 in the pH 12 buffer. Note that at 40°C, steady-state concentrations for each component appear to have been reached with the first sampling that was taken at 4 days. Similar behavior is observed at 90°C except that the Na concentrations appear to be elevated at the earliest sampling. Figure 4 shows the elemental release data for glass L7-15 in the pH 9 buffer. Concentrations at the lower pH are lower due to the slower reaction kinetics at pH 9, but the trends in the release behavior of the major glass components appear essentially identical to the trends observed for LD4-9012 glass in the pH 12 buffer.

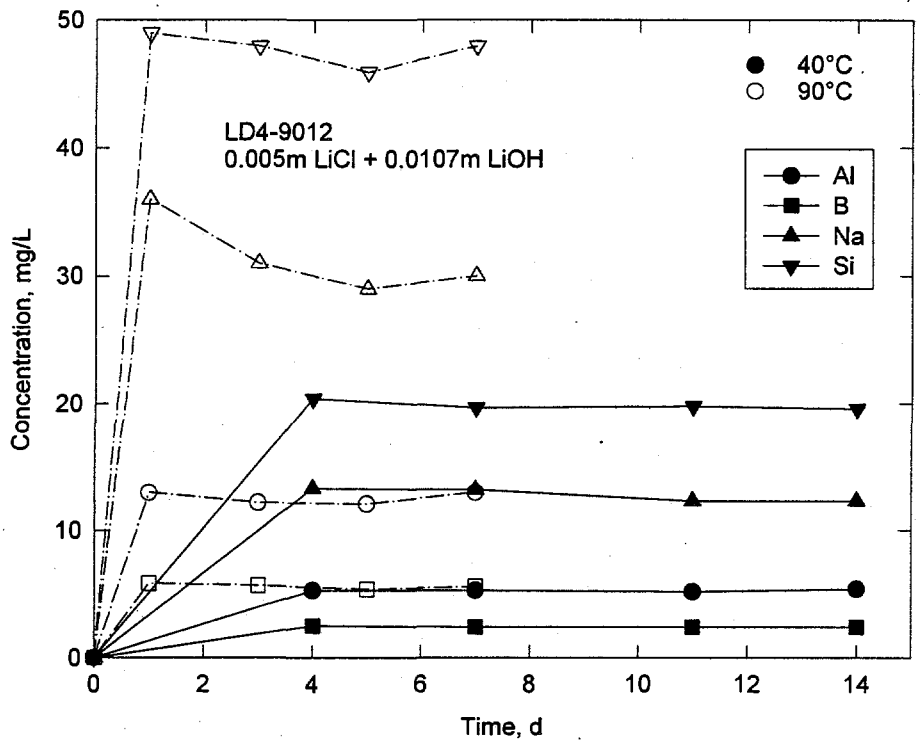

Figure 3. Concentration of Major Glass Components Released From LD4-9012 Glass as a Function of Time

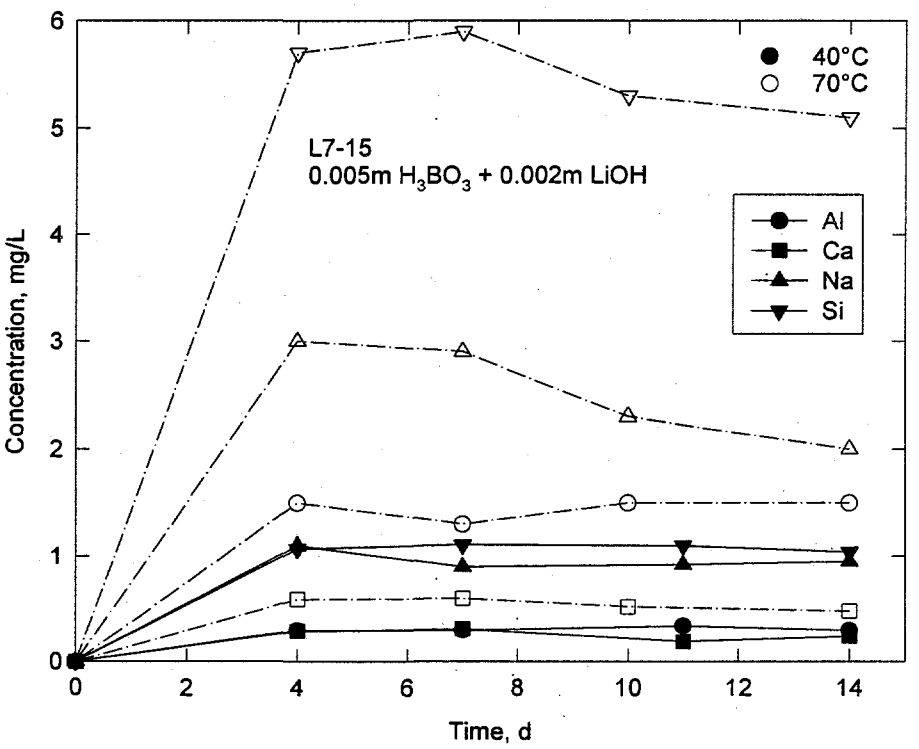

Figure 4. Concentration of Major Glass Components Released From L7-15 Glass as a Function of Time

CORROSION RATE RESULTS

Tables 5 and 6 give the mean and standard deviation of the corrosion rate for each glass that was computed with the SIPFT code. The data taken at the first sampling were excluded in calculating the mean and standard deviation. Selected results are presented here to again illustrate trends in the corrosion rate data that were common among the six glasses tested.

Figure 5 shows the calculated normalized release rate data in the pH 9 buffer for LD6-5412 glass. Except for Na at early times, all the glass elements were released essentially stoichiometrically, indicating congruent dissolution. Figure 6 shows the calculated normalized release rate from the SRM622 glass in the same pH 9 buffer. Note that at 70°C, the Al release falls rapidly to below detection limits after the 10th day of the test indicating that a secondary phase may have

Table 5. Mean Corrosion Rates ($g/m^2 \cdot d$) For the Six LAW Test Glasses at 40, 70, and 90°C in the 0.005m H_3BO_3 + 0.002m LiOH Buffer Solution

Glass ID	Al	Ca	Na	Si
	-0.0024 ±0.0082		0.0112 ±0.0016	0.0038 ±0.0007
LD4-9012	0.0760 ±0.0060		0.0592 ±0.0074	0.0554 ±0.0009
	0.2445 ±0.0326		0.2750 ±0.0359	0.2282 ±0.0188
	-0.0099 ±0.0001	0.0068 ±0.0029	0.0130 ±0.0013	0.0086 ±0.0002
LD6-5412	0.0735 ±0.0080	0.0486 ±0.0010	0.0748 ±0.0030	0.0675 ±0.0046
	0.2111 ±0.0182	0.2918 ±0.0791	0.2262 ±0.0273	0.2085 ±0.0178
	0.0070 ±0.0004	0.0050 ±0.0030	0.0120 ±0.0004	0.0052 ±0.0003
L7-15	0.0726 ±0.0063	0.0410 ±0.0064	0.0713 ±0.0137	0.0627 ±0.0048
	0.1912 ±0.0125	0.2878 ±0.0626	0.2257 ±0.0096	0.1907 ±0.0052
	0.0073 ±0.0173	0.0033 ±0.0025	0.0519 ±0.0070	0.0092 ±0.0011
L7-25	0.1043 ±0.0044	0.0185 ±0.0013	0.1766 ±0.0239	0.0765 ±0.0036
	0.3339 ±0.0293	0.2107 ±0.1092	0.8299 ±0.3390	0.3369 ±0.0266
	-0.0094 ±0.0001	0.0097 ±0.0034	0.0164 ±0.0059	0.0117 ±0.0017
SRM622	0.0307 ±0.0844	0.0571 ±0.0065	0.0631 ±0.0085	0.0602 ±0.0062
	0.1842 ±0.0192	0.2455 ±0.0045	0.2332 ±0.0125	0.2414 ±0.0070
	-0.0110 ±0.0018	0.0039 ±0.0032	0.0209 ±0.0029	0.0047 ±0.0005
L8-3	0.0619 ±0.0165	0.0310 ±0.0024	0.0893 ±0.0130	0.0505 ±0.0029
	0.1770 ±0.0124	0.2823 ±0.0983	0.2944 ±0.0577	0.1662 ±0.0088

Table 6. Mean Corrosion Rates ($g/m^2 \cdot d$) For the Six LAW Test Glasses at 40, 70, and 90°C in the 0.005m LiCl + 0.0107m LiOH Buffer Solution

Glass ID	Al	B	Ca	Na	Si
	0.1278 ±0.0024	0.1223 ±0.0039		0.1322 ±0.0063	0.1164 ±0.0029
LD4-9012	0.5190 ±0.0271	0.4180 ±0.0506		0.5565 ±0.0384	0.5113 ±0.0292
	0.9379 ±0.0486	0.6167 ±0.0902		1.0048 ±0.0701	0.8650 ±0.0248
	0.1209 ±0.0028	0.1101 ±0.0031	0.0935 ±0.0032	0.1269 ±0.0025	0.1073 ±0.0016
LD6-5412	0.3491 ±0.0086	0.3832 ±0.0172	0.1660 ±0.1099	0.3895 ±0.0200	0.3480 ±0.0152
	0.6446 ±0.0919	0.6354 ±0.0466	0.3174 ±0.1215	0.8049 ±0.1333	0.5995 ±0.0727
	0.1077 ±0.0064	0.0064 ±0.1101	0.0586 ±0.0017	0.1139 ±0.0038	0.0969 ±0.0028
L7-15	0.3495 ±0.0117	0.0117 ±0.3832	0.1657 ±0.0029	0.4041 ±0.0200	0.3395 ±0.0143
	0.6006 ±0.0591	0.0591 ±0.6354	0.2880 ±0.0383	0.8146 ±0.1021	0.5893 ±0.0470
	0.1674 ±0.0109	0.1801 ±0.0054	0.0476 ±0.0008	0.1796 ±0.0097	0.1575 ±0.0044
L7-25	0.5425 ±0.0557	0.6060 ±0.0575	0.0653 ±0.0085	0.7212 ±0.0424	0.5295 ±0.0432
	1.1375 ±0.0787	1.2459 ±0.0793	0.0541 ±0.0092	2.0305 ±0.4142	1.1018 ±0.0658
	0.1075 ±0.0373		0.0508 ±0.0517	0.1360 ±0.0055	0.1095 ±0.0033
SRM622	0.2613 ±0.0110		0.0879 ±0.0047	0.9229 ±0.0619	0.6387 ±0.0529
	0.3169 ±0.0161		0.1070 ±0.0090	2.1517 ±0.0602	1.4273 ±0.0381
	0.0729 ±0.0056	0.0071 ±0.0189	0.0103 ±0.0012	0.0771 ±0.0043	0.0577 ±0.0032
L8-3	0.3301 ±0.0059	0.2250 ±0.0346	-0.0037 ±0.0046	0.4130 ±0.0095	0.2936 ±0.0152
	0.8419 ±0.0159	0.8127 ±0.0374	0.0172 ±0.0037	1.1203 ±0.0464	0.7557 ±0.0337

formed that is removing Al from solution. The 90°C data also show incongruent release of Al throughout the entire test. As will be shown in the following section, secondary phase formation may have affected the results from the test with this glass.

Figures 7 and 8 show a comparison of the normalized Si release rate for each of the six test glasses in the pH 9 and pH 12 buffers, respectively. Little difference in the forward reaction rate is observed for the test glasses in the pH 9 buffer solution. However, glass composition has much more effect on the rates in the pH 12 buffer. As expected, the L7-25 glass with the highest Na_2O content gave the highest forward rate and the L8-3 glass that contains 3 wt% ZrO_2 the lowest rate, particularly at the lower temperature.

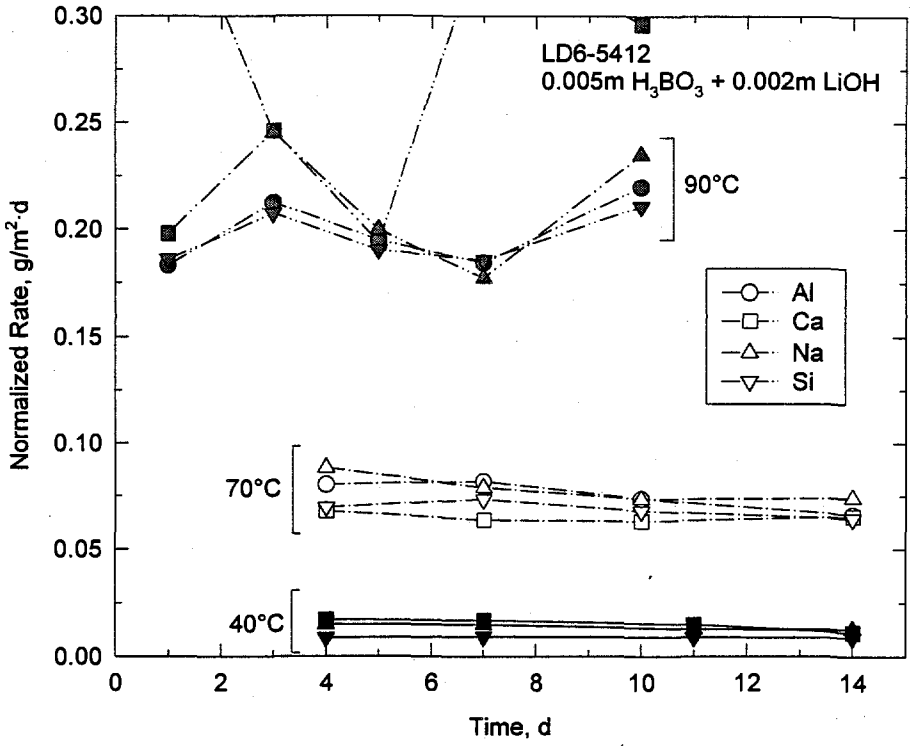

Figure 5. Normalized Release Rate of Major Components From LD6-5412 Glass as a Function of Time and Temperature

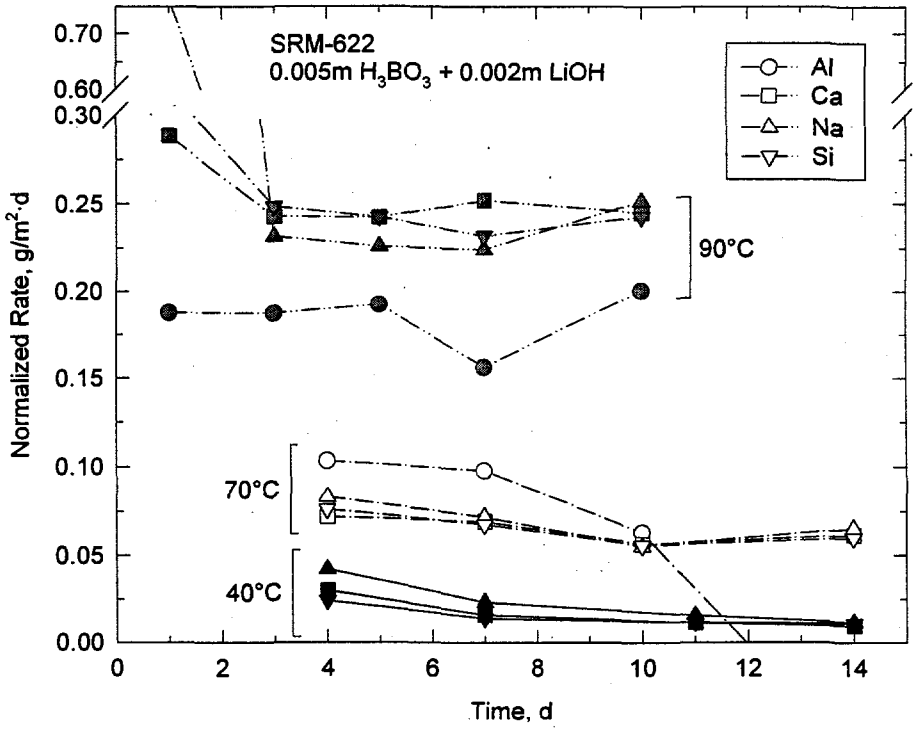

Figure 6. Normalized Release Rate of Major Components From SRM622 Glass as a Function of Time and Temperature

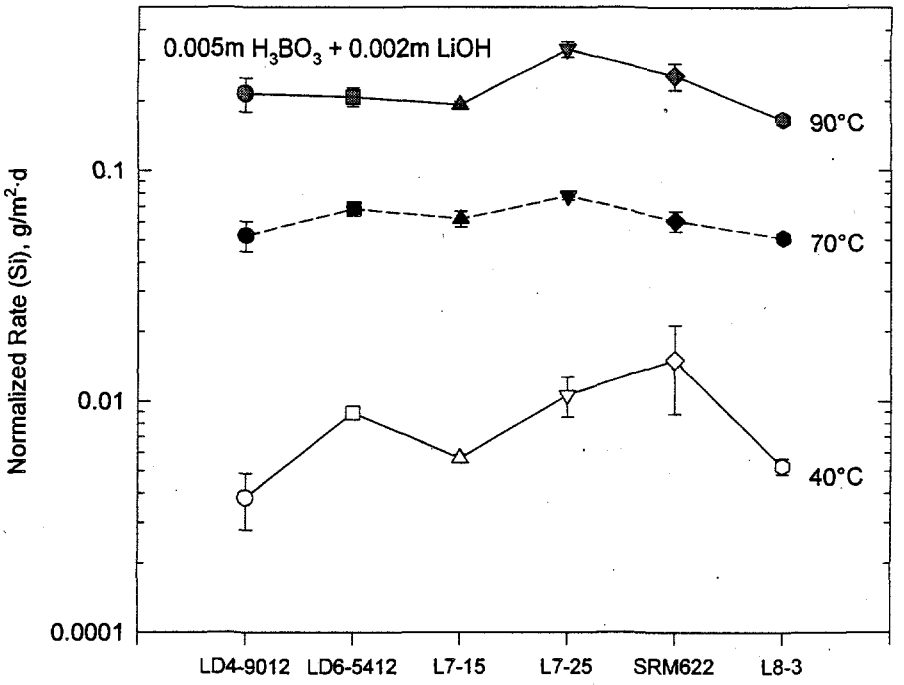

Figure 7. Comparison of Normalized Si Release Rate for the Six Test Glasses in the pH 9 Buffer Solution

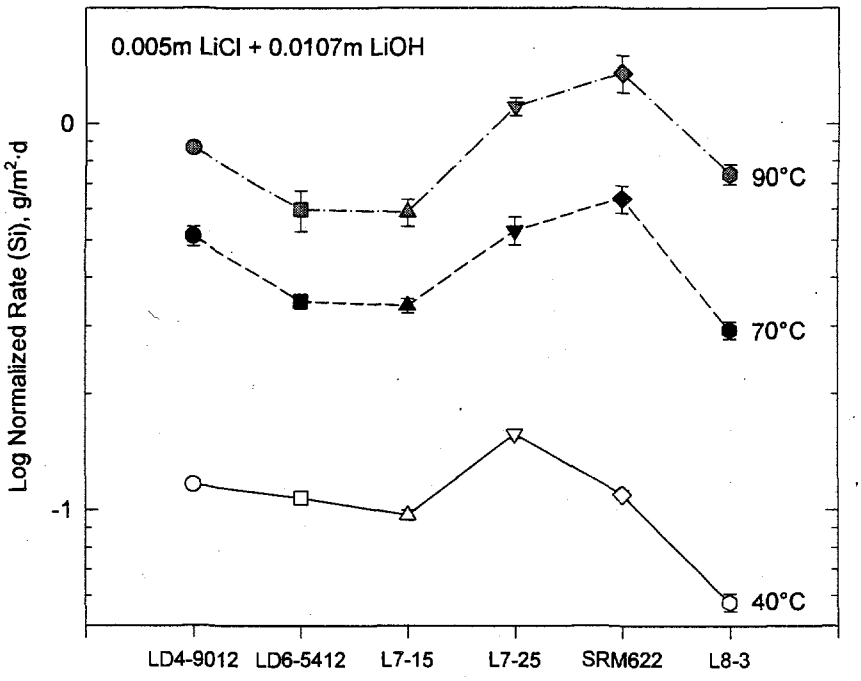

Figure 8. Comparison of Normalized Si Release Rate for the Six Test Glasses in pH 12 Buffer Solution

DISCUSSION

The data presented in the previous section demonstrate that the SPFT method can be used to accurately measure changes in the corrosion rate of silicate glasses as a function of glass composition. As such, we have shown that the method is suitable as an acceptance test for a LAW product specification. However, we have not yet proven that the corrosion rate measured in these tests is the true so-called "forward rate" of reaction.

GEOCHEMICAL CODE SIMULATIONS

Assuming that the following equation adopted from the work of Agaard and Helgeson for the corrosion of silicate minerals in water applies equally well to silicate glass/water systems, we have

$$k = k_o 10^{\eta(\mathrm{pH})} e^{\frac{E_a}{RT}} \left[1 - \frac{Q}{K}\right] \tag{3}$$

where k = corrosion rate, $g/m^2 \cdot d$
k_o = intrinsic rate constant, $g/m^2 \cdot d$
η = power law coefficient for solution pH
E_a = activation energy, cal/mol
R = gas constant, cal/mol·K
T = temperature, K
Q = ion activity product
K = pseudoequilibrium constant.

The term in brackets in Equation (3) is usually referred to as the "chemical affinity" term as it is a measure of the overall affinity for the conversion of the glass into more stable products. The variable K is a pseudoequilibrium constant because silicate glasses are not thermodynamically stable in water and so equilibrium between glass and water cannot exist. Consequently, the chemical affinity for glass dissolution is approximated by an appropriate solid phase. Identification of the appropriate solid phase is an ongoing area of research and discussion among glass scientists. There is evidence to support the use of SiO_2 polymorphs (Advocat et al. 1990) and more complicated mineral assemblages (Bourcier et al. 1990). The appropriate solid phase to use for LAW glass must be determined from laboratory tests and comparisons of modeling simulations

with laboratory data. For the purposes of this report, it will be assumed that the chemical affinity term can be reasonably approximated by amorphous silica.

In the SPFT test, the goal is to maintain dilute solution conditions such that $Q/K \approx 0$. If this condition is true, then the chemical affinity term can be dropped from Equation (3) giving

$$\vec{k} = k_o 10^{\eta(\mathrm{pH})} e^{\frac{E_a}{RT}} \tag{4}$$

where $\vec{k}$ = forward reaction rate, g/m^2·d. The parameter Q/K, or saturation index, was computed for the conditions of the SPFT tests with the aid of the geochemical code EQ3/6 (Wolery 1992). Figure 9 shows a typical result for glass LD4-9012. The vertical line is the maximum value of reaction progress achieved in the SPFT test that was calculated from the maximum concentration of Si measured in the effluent. The horizontal line is drawn at a log $Q/K = 0$ indicating saturation with respect to a solid phase. The curves are the computed saturation indices for each mineral phase assuming the glass dissolves congruently in the aqueous phase. Sodium was found to be preferentially released at early times in our experiments, so this computational procedure will

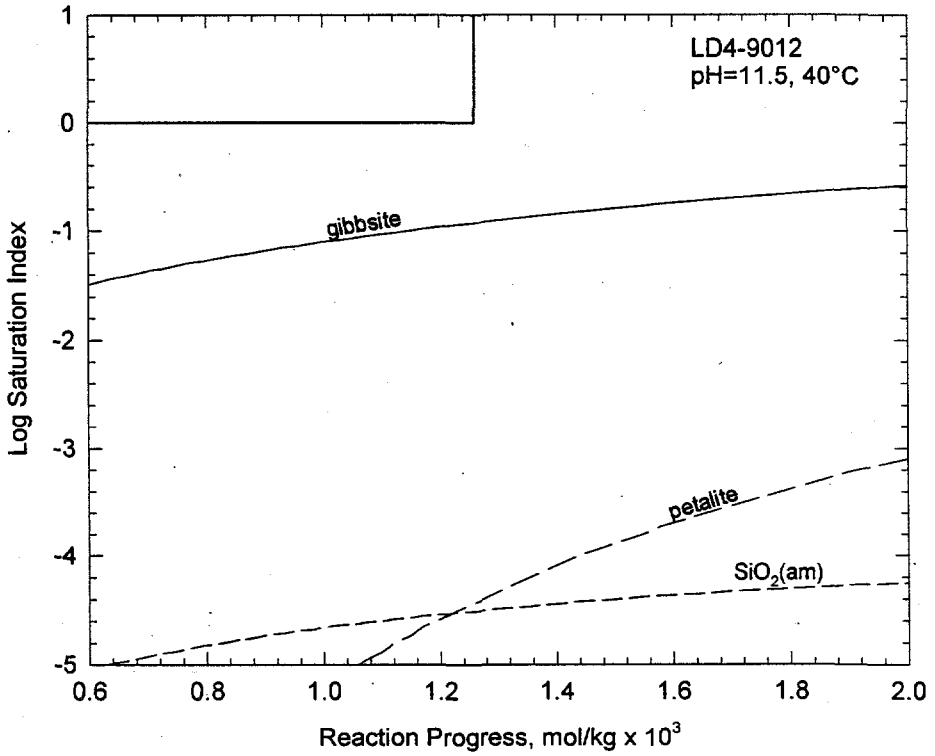

Figure 9. Calculated Saturation Indices for Selected Mineral Phases in a SPFT Test with LD4-9012 Glass in 0.005m LiCl + 0.0107m LiOH Solution at 40°C

underestimate the saturation indices for solid phases that contain Na. However, almost all of these phases were many orders of magnitude undersaturated, so correcting for the early-time, incongruent release of Na was not considered important. Curves falling inside the box indicate supersaturation with respect to the phase and thus the *potential* for precipitation of the phase in the experiment. Careful interpretation of these calculations is required because many factors contribute to the nucleation and growth of a secondary phase, including kinetic constraints on precipitation. Also, at temperatures ≥40°C, direct measurement of the solubility products for minerals in the database is sparse. Extrapolation techniques are then used to compute equilibrium constants, which increases the uncertainty in the computed saturation indices. Still, the calculations provide an extremely useful, if not fully quantitative, analysis of whether the desired conditions of the SPFT test were actually achieved.

For the test shown in Figure 9, there are no mineral phases that compute as supersaturated, indicating that the release rate of all the glass components should be congruent. Figure 10 shows that, indeed, this is the case. Even more importantly, the saturation index of SiO_2(am) is $<10^{-4}$. If the saturation index of this phase approximates the chemical affinity term in the rate equation

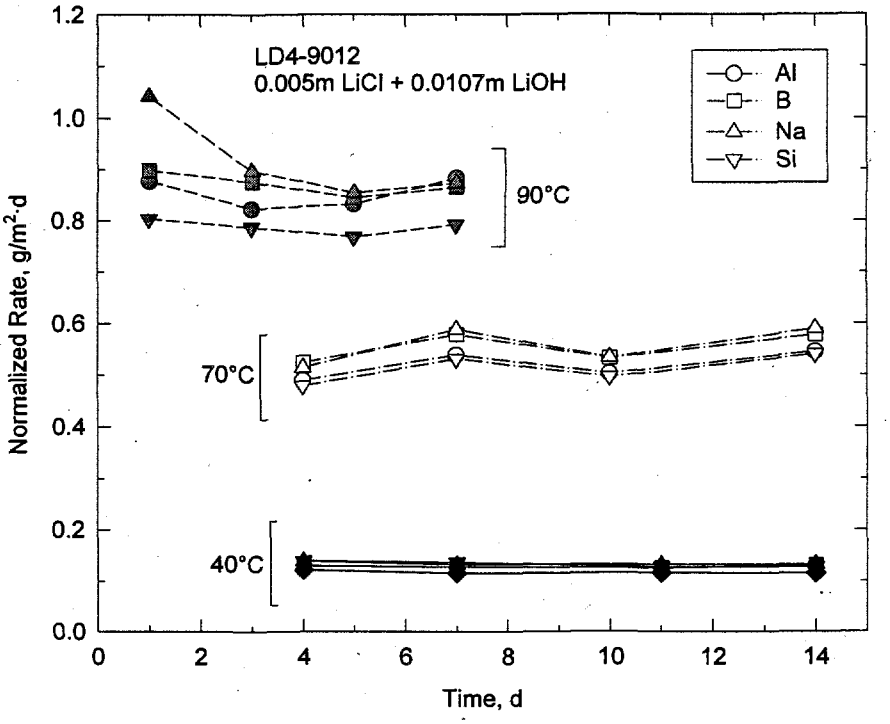

Figure 10. Normalized Release Rate as a Function of Time For Glass LD4-9012 in pH 12 Buffer Solution

(3) to within even two orders of magnitude, the rate measured in the SPFT test is the true "forward rate" because the condition $Q/K \approx 0$ has been met.

Figure 11 shows the calculated saturation indices for LD6-5412 glass in the pH 9 buffer at 90°C. Several additional mineral phases appear because this glass contains approximately 4 wt% CaO. The most supersaturated is hydroxylapatite [$Ca_5OH(PO_4)_3$], followed by the zeolite mesolite [$Na_{0.676}Ca_{0.657}Al_{11.99}Si_{3.01}O_{10}{\cdot}2.65H_2O$] and scolecite [$CaAl_2Si_3O_{10}{\cdot}3H_2O$]. To check if the precipitation of these phases was consistent with the solution composition data, the calculation was repeated but this time allowing the code to precipitate these phases and thus impact the solution concentration of Na, Ca, Al, and Si. The calculated concentration of each element in this case was much lower than the measured values. Consequently, it is highly unlikely that these secondary phases formed in the test, and the corrosion rates calculated from the data should be reliable.

Figure 12 shows the calculated saturation indices for the SRM622 glass. This glass had the highest CaO loading of any of the glass compositions tested and also contains 166 times more

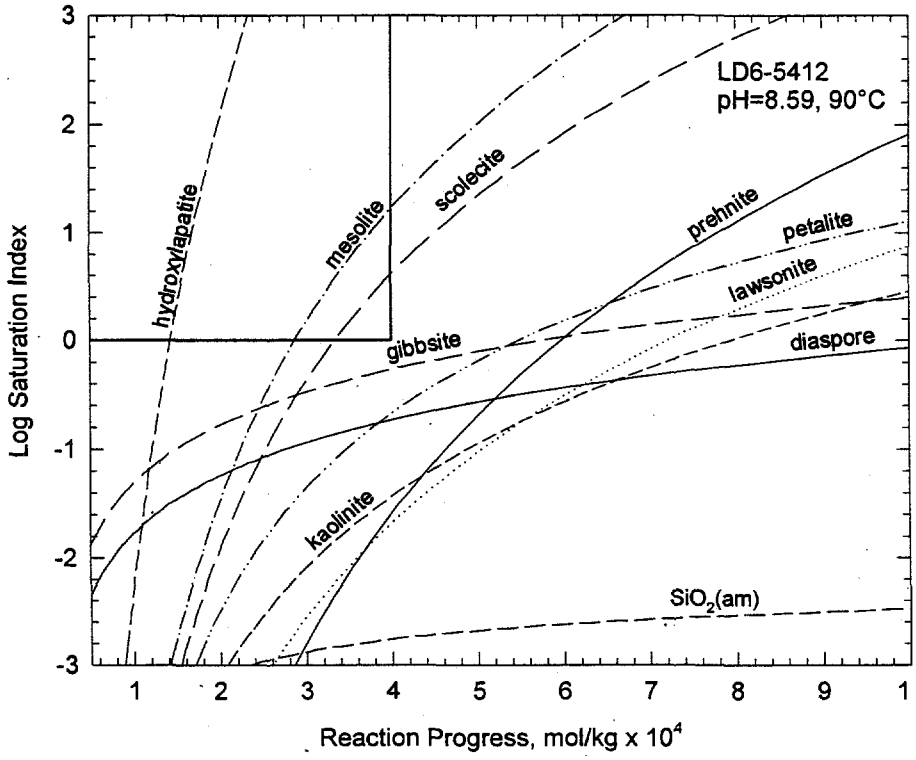

Figure 11. Calculated Saturation Indices for Selected Mineral Phases in a SPFT Test with LD6-5412 Glass in 0.005m H_3BO_3 + 0.002m LiOH Solution at 90°C

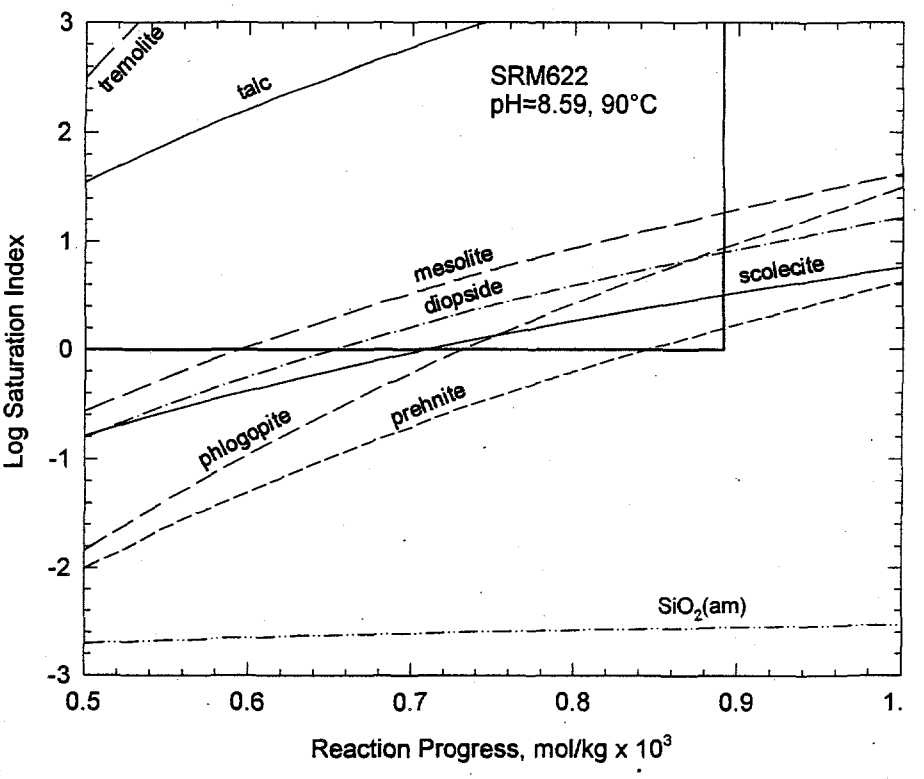

Figure 12. Calculated Saturation Indices for Selected Mineral Phases in a SPFT Test with SRM622 Glass in 0.005m H_3BO_3 + 0.002m LiOH Solution at 90°C

Mg than the reference LAW glasses, although the relative mass fraction of MgO is still small compared with the other major glass components. The result, as illustrated in Figure 12, is that significantly more secondary phases were calculated to be supersaturated in the SPFT tests with this glass. The corrosion rates calculated for this glass were also distinct from the other glasses tested in that the rates decreased uniformly with time at each temperature. Because a significant number of phases were calculated as supersaturated, and because of the unusual time-dependence observed with this glass, we conclude that the data from this test may be unreliable. It is recommended that this test be repeated with a lower glass surface area or higher flow rate to ensure that the system remains undersaturated with respect to the major mineral phases shown in Figure 12.

KINETIC RATE PARAMETERS

In this study, only 2 pH values and 3 temperatures were evaluated. This data set is inadequate to accurately compute the kinetic rate parameters in Equation (4) using nonlinear regression techniques. However, one of the test glasses in this study (LD6-5412) is being fully tested

over a range of pH values and temperatures as part of a LAW glass development and testing program at PNL. By combining the data obtained from this study with the tests run independently, sufficient data are available for the LD6-5412 glass to compute the kinetic rate constants.

Figure 13 shows the measured glass corrosion rate based on the normalized Si release rate as a function of the computed pH at temperature for each of the buffer solutions used. The η values shown were calculated from a linear regression to the data at each temperature. The data indicate that the pH-dependence of the rate decreases slightly with increasing temperature. Using the regressed η values, a nonlinear regression was performed using Equation (4) and the entire SPFT data set with the exception of the data at 40°C and pH 5.9. The results gave values for log k_o= 10.2 ±0.3 g/m^2·d and E_a = 22.3 ±0.4 kcal/mol. These values are consistent with many previous studies of silicate glass/water reaction.

There is not yet a satisfactory explanation for the pH dependence of the corrosion rate measured in SPFT tests. However, the rate most likely depends on concentration of oxo, hydroxo, and aquo sites at the surface of the glass that vary as a function pH and temperature. A study is

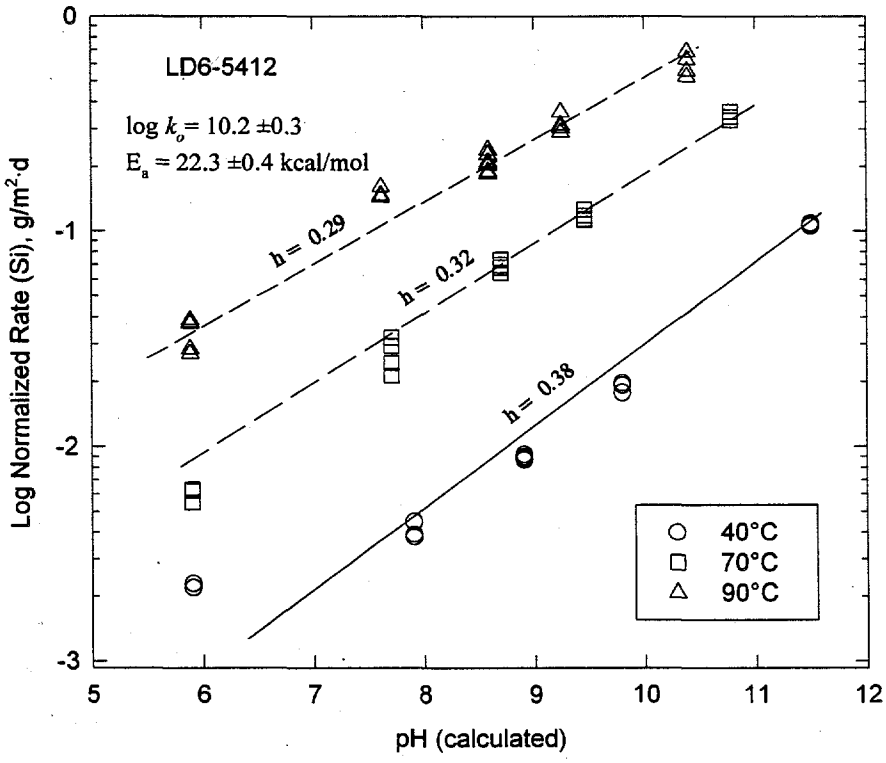

Figure 13. Normalized Si Release Rate as a Function of pH for LD6-5412 Glass. Lines were calculated from Equation (3) using the regressed parameters shown.

planned in the near future at PNL to utilize recent advances in computerized molecular mechanics to predict stability constants for proton binding at oxide surfaces (Rustad and Hay 1995). With these stability constants, it is hoped that pH dependence of the rates observed in the SPFT test can be predicted from first principles.

INTERLABORATORY DISCREPANCY IN SPFT RESULTS

As was noted in the Introduction, a set of SPFT tests was also conducted at ANL to facilitate comparison of results because the SPFT procedures used at ANL are distinctly different from those used in this study. The flow-through tests run at ANL were done on glasses L8-3 and SSHTM-3, a glass that is essentially identical to the LD6-5412 composition tested at PNL.[a] The ANL tests were run at 20°C and 40°C so direct comparison is only possible with the 40°C data. Figure 14 summarizes the results from the two laboratories. The corrosion rates measured at ANL are approximately 30 to over 1000 times larger than the values measured at PNL. Such a large difference is extremely troubling because it casts doubt on whether either laboratory is accurately measuring the forward rate.

The first question to be answered is whether the results from either laboratory are consistent with forward rate data obtained from independent sources. One such data set was obtained at Lawrence Livermore National Laboratory for a glass of very similar composition to the LAW glasses tested in this study. Knauss et al. (1990) conducted SPFT tests at 25, 50, and 70°C with a 5 component glass of the composition 18.2 wt% Na_2O, 5.97 wt% CaO, and 11.68 wt% Al_2O_3, 8.43 wt% B_2O_3, and 55.73 wt% SiO_2. At 70°C and pH 10.8 (at temperature pH), Knauss et al. report a forward rate of approximately 0.2 $g/m^2 \cdot d$. This rate is consistent with the range of values we have measured for the 20 wt% Na_2O LLW glasses (see Table 6). Knauss et al. also reported that the release of glass components was stoichiometric at this pH. Stoichiometric release of the glass components was also found in our tests at this pH for most of the glasses. Another forward rate data set is available from Soxhlet tests performed by Delage and Dussossoy (1991).

[a]Although not reported here, SPFT tests were run at PNL with SSHTM-3 glass and the corrosion rate was found to be identical, within experimental error, to LD6-5412 glass.

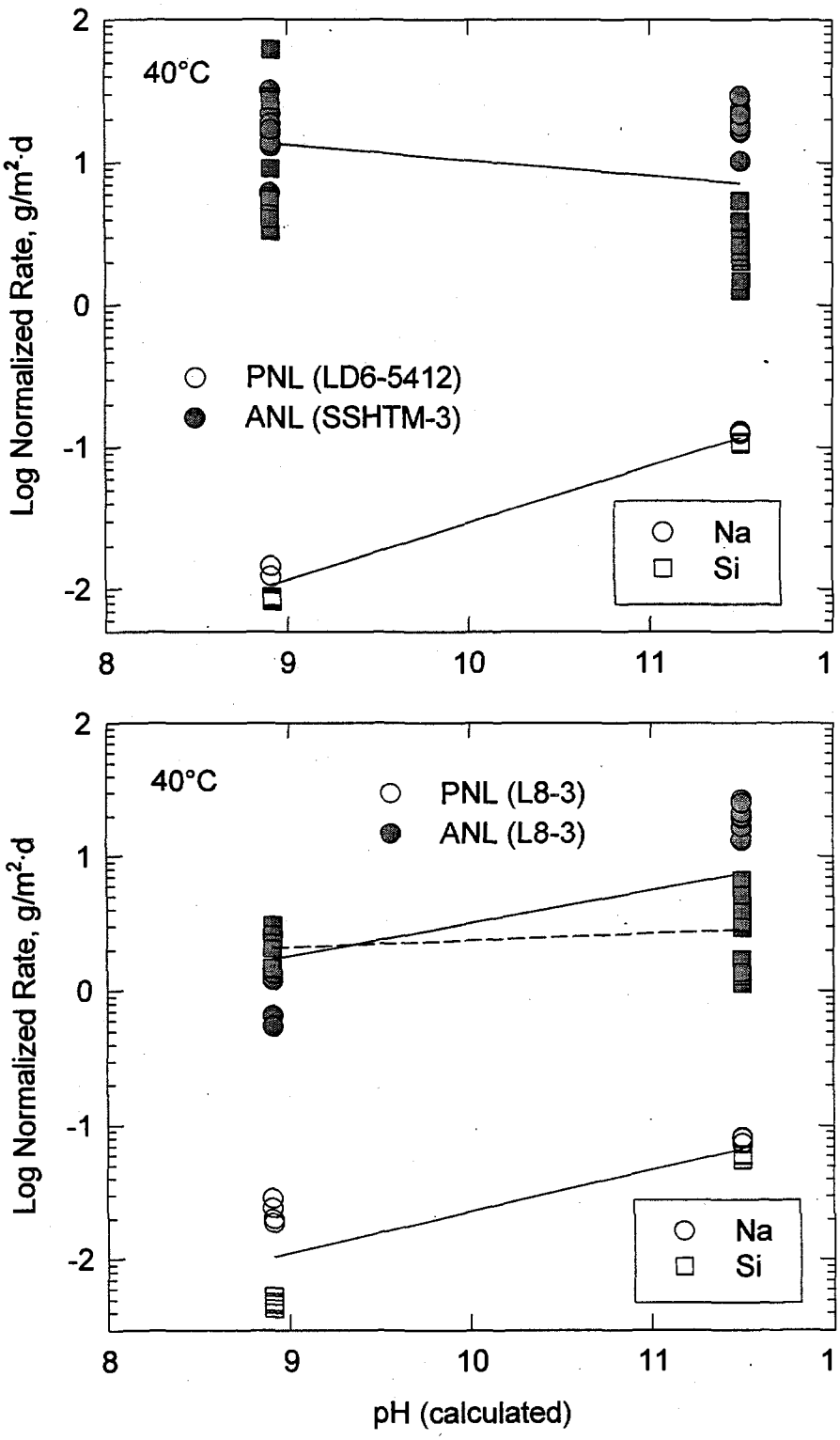

Figure 14. Comparison of SPFT Results on Two LAW Glasses at 40°C. Lines shown are simple linear regressions through the data with the dashed line a regression for the ANL data for Si only.

They reported forward rates for a HLW glass formulation (R7T7) on the order of 1 $g/m^2 \cdot d$ at a temperature of 90°C. As shown in Figure 13, the PNL forward rate values for LD6-5412 glass at 90°C are of this same order of magnitude. Qualitatively, our data are consistent with these independent studies while the ANL results are not.

Next, a simple linear regression was performed on the data from both laboratories to determine the pH-dependence of the rate (see Figure 14). Because of the large amount of scatter in the ANL data set, it is impossible to determine a statistically meaningful pH dependence for the rate. The simple linear regression to the ANL data gives corrosion rates based on Si release that are either pH-independent or *decrease* with increasing pH. This result is inconsistent with the fundamental physical chemistry of the glass-water reaction. As is shown in Figures 13 and 14, the PNL flow-through results give a consistent data set with the measured rate increasing with increasing pH.

Figure 15 shows normalized release of B, Na, and Si from SSHTM-3 glass in the short-term, low S/V, PCT tests done at ANL. The data at $S/V \cdot t > 3000$ d/m clearly show evidence of solution chemical effects that are changing the glass reaction rate. A linear regression on the data for $S/V \cdot t < 3000$ d/m gave a value for the intercept of 1.24 ± 1.21 g/m^3, indicating no statistical significance to including the intercept in the regression; i.e., the line through these data also passes through the origin. This result is significant because it indicates that the PCT data for $S/V \cdot t < 3000$ m^{-1} can be used to approximate the forward reaction rate. Using a simple $y = A \cdot x$ model, the value for the slope is 0.0079 ± 0.0002 $g/m^2 \cdot d$. The pH in the PCT test will vary between a starting value of approximately 8.5 and a final pH that varies with the test duration. For the tests with $S/V \cdot t < 3000$ d/m, the final pH at room temperature was measured at between 9.2 and 9.7. At 40°C, the in situ pH is approximately 0.3 to 0.4 pH unit lower than at room temperature so the pH in the PCT tests varies from an initial value of approximately 8 to a final value of 8.8 to 9.4. Using the regressed coefficients calculated from the PNL flow-through data shown in Figure 13 and Equation (4), the computed forward rate for this pH range in the PCT is 0.005 to 0.016, which is consistent with the forward rate approximated from the PCT data.

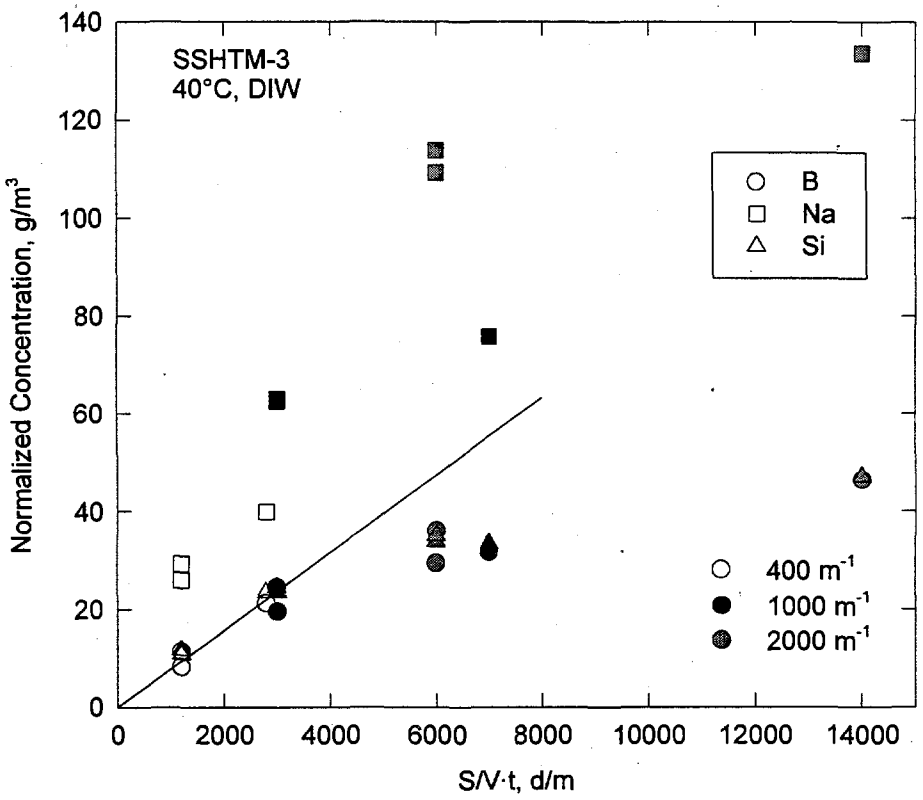

Figure 15. Normalized Release of Selected Elements From SSHTM-3 Glass in 400 m^{-1} PCT Tests. The line is from a linear regression to the equation $y = A \cdot x$ using the data for $S/V < 3000$ m^{-1}.

Because the ANL flow-through results gave forward rate values that are nearly two orders of magnitude larger than the PNL values, it is impossible to model the PCT results using these data and Equation (4), where the chemical affinity term $(1-Q/K)$ has been assumed to be near zero. So, numerical integration of Equation (3) was performed using the IPAI code (see Appendix C) and a variety of different mineral phases were evaluated as a control for the chemical affinity. While it was possible to adjust equilibrium constants to compute corrosion rate values that were approximately correct for the 3-day, 400-m^{-1} results, the simulations were unsatisfactory in that the computed solution concentrations of the glass components were not consistent with the measured data. Reducing the chemical affinity of the reaction by a factor of over 100 resulted in the precipitation of insoluble mineral phases that controlled the concentration of Al, Na, Ca, and Si to values much lower than were measured in the PCT tests. Including Al and Ca species activities directly in the rate equation was also tried as a means to reduce the reaction rate. It was possible to adjust the power law coefficients to obtain a reasonable fit to the 3-day, 400-m^{-1} re-

sults, but the simulations were again unsatisfactory in that the calculated rate falls much too quickly to accurately reproduce the PCT results at larger values of S/V·t. We were not able to find any combination that gave satisfactory results.

From the discussion above, we conclude that the forward rate values reported by ANL are not correct. If this conclusion is valid, then the source(s) of the differences in the results between the two laboratories must still be explained. There are differences in data analysis and test procedures used at both laboratories. These differences will be examined below as possible sources of the discrepancy.

Data Analysis

As indicated in the Experimental section, glass corrosion rates were computed from the flow-through data obtained at PNL using the following equation:

$$R_{i,j} = (C_{i,j} - \overline{C}_{i,b})\frac{Q_j}{f_i S_j}.$$

In contrast, Ebert et al. (1995) reported that their glass corrosion rates were computed from the following equation

$$R_{i,j} = C_{i,j}\frac{Q_j}{f_i S_o}. \qquad (5)$$

The differences that result from using Equation (5) versus Equation (1) to compute a glass corrosion rate are 1) the data are not background corrected, and 2) time-dependent changes in the glass surface area are not taken into account. Given the short duration of the ANL experiments (< 1 day), accounting for the time-dependent change in the glass surface area would have only a small (<20%) effect on the computed corrosion rates. However, as we will demonstrate, neglecting background subtraction can have a significant effect on the computed corrosion rates.

First, it is instructive to calculate the minimum observable glass corrosion rate based only on the background concentration of the glass components. For purposes of illustration, we will focus the remaining discussion on one glass component, Si, and use the data from the pH 12 buffer solution (0.005m LiCl + 0.0107m LiOH). No background concentration data were reported by

Ebert et al. (1995), so the PNL data will be used. From the PNL database, the mean background Si concentration in the pH 12 buffer is 0.126 ±0.025 g/m^3. The minimum detectable rate is then given by

$$R_{min} = (\overline{C}_{i,b} \pm \sigma)\frac{Q_j}{f_i S_o}. \quad (6)$$

The solid lines in Figure 16 show the calculated range in R_{min} as a function of Q/S for SSHTM-3 glass using the background concentration of Si given above. As is apparent from Figure 16 and by simple inspection of Equation (6), the minimum detectable rate given a constant background concentration, increases linearly with increasing flow rate and/or decreasing glass surface area. Also plotted on Figure 16 are the reported corrosion rate data from ANL and PNL where the position along the abscissa was determined by the flow rate and glass surface area used in the tests at both laboratories. It is immediately apparent from the data in Figure 16 that both the magnitude and scatter in the ANL corrosion rate data are within the expected range of rates that would be computed just from the background concentration, assuming that the background con-

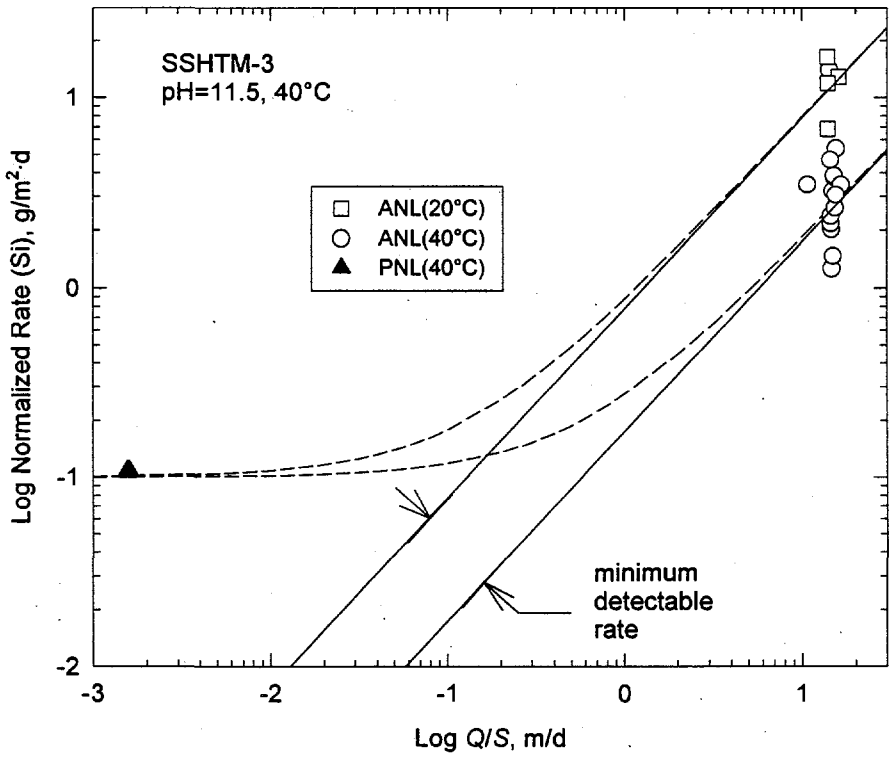

Figure 16. Minimum Detectable Rate as a Function of Q/S Based on Background Concentration of Si in SPFT Tests. Dashed lines were extrapolated from PNL SPFT data neglecting background subtraction.

centration measured in the PNL tests is similar in the ANL tests. If we further assume that the glass corrosion rate is independent of the flow rate at the PNL test conditions, Figure 16 shows the effect of increasing flow on the corrosion rate computed without background subtraction. Because the Si solution concentration contributed from glass corrosion decreases as the flow rate increases, the contribution to the calculated rate from the background concentration increases until, eventually, it is impossible to distinguish the true rate from the background rate. The data in Figure 16 clearly indicate the importance of applying background subtraction to the solution concentration data when running SPFT experiments at the very high flow rates.

Test Procedures

Another key difference in the SPFT test procedures used at ANL and PNL is that the ANL procedure calls for short-duration (hours) and very high-flow rate while the PNL procedure calls for slow or intermediate flow rate and "long-duration" (days to weeks). As was discussed previously, as long as the flow rate is sufficiently high to maintain dilute solution conditions, flow rate differences should not affect the results. The differences in the duration of the experiments, however, almost certainly has an effect. In the experiments reported on here, both laboratories used glass that was prepared according to standard PCT methods. Crushing and grinding of the glass results in the formation of some fine grained material that adheres to the glass surfaces and is not removed during the cleaning steps. The exposed surfaces of the glass grains also contain numerous ridges that result from brittle fracture. These structures have a high strain energy and are thought to be more readily susceptible to aqueous attack.

The early stages of the glass reaction with water are also dominated by the exchange of alkali ions exposed on the fracture surfaces. In static tests, this process results in enhanced normalized release of Na at early times that increases proportionally with the S/V of the test, as is clearly evident in Figure 15. The combined effect of all of these processes is that corrosion rates measured in short-duration experiments, especially on the order of hours, are unreliable. Consequently, it is difficult to justify short-duration experiments for an accurate measurement of the bulk glass dissolution rate that is being sought with the SPFT test.

CONCLUSION

Overall, we have found that using the PNL SPFT procedure, one can quantitatively distinguish reaction rate differences as a function of glass composition, temperature, and pH. The ability to discriminate among glass compositions appears to be equivalent to the PCT without the time-varying solution chemistry that complicates the interpretation of PCT results. We conclude that the PNL SPFT test procedure meets all of the requirements for an acceptance test for LAW glasses. Using the SPFT test as an acceptance test has the added benefit that the test provides data that can be directly used in a computer code that has been selected for performance assessment analyses of the Hanford LLW disposal system (McGrail and Mahoney 1995).

Discrepancies in the results from SPFT testing conducted at ANL and PNL on the same glasses were examined and found to be due to differences in the data analysis and test procedures used. Neglecting background subtraction in computing corrosion rates from the ANL SPFT tests conducted at high flow rate appears to be a major source of the discrepancy. The short-duration of the ANL tests is also thought to be a factor contributing to the much higher corrosion rate values reported from those tests. Modeling simulations showed that the PNL forward rate measurements were consistent with forward rate values estimated from short-time, low surface-area-to-volume ratio PCT data and were successfully used to reproduce the glass/water reaction kinetics observed in the PCT. Geochemical reaction path simulations were also used along with the ANL forward rate data to model the PCT results. All attempts to reproduce the PCT results with the ANL data and the full kinetic rate equation for the glass-water reaction were unsuccessful.

REFERENCES

Advocat, T., J. L. Crovisier, B. Fritz, and E. Vernaz. 1990. "Thermokinetic Model of Borosilicate Glass Dissolution: Contextual Affinity." In *Scientific Basis for Nuclear Waste Management XIII*, eds. V. M. Oversby and P. W. Brown, Materials Research Society, Pittsburgh.

Bates, J. K. C. R. Bradley, E. C. Buck, J. C. Cunnane, W. L. Ebert, X. Feng, J. J. Mazer, D. J. Wronkiewicz, J. Sproull, W. L. Bourcier, B. P. McGrail, and M. K. Altenhofen. 1994. *High-Level Waste Borosilicate Glass: A Compendium of Corrosion Characteristics*. DOE-EM-0177, U.S. Department of Energy, Office of Waste Management, Washington, D.C.

Bourcier, W. L., D. W. Peiffer, K. G. Knauss, K. D. McKeegan, and D. K. Smith. 1990. "A Kinetic Model for Borosilicate Glass Dissolution Based on the Dissolution Affinity of a Surface Alteration Layer." In *Scientific Basis for Nuclear Waste Management XIII*, eds. V. M. Oversby and P. W. Brown, Materials Research Society, Pittsburgh.

Delage, F., and J. L. Dussossoy. 1991. "R7T7 Glass Initial Dissolution Rate Measurements Using a High-Temperature Soxhlet Device." In *Scientific Basis for Nuclear Waste Management XIV*, eds. T. Abrajano, Jr. and L. H. Johnson, Materials Research Society, Pittsburgh.

Knauss, K. G. and T. J. Wolery. 1986. "Dependence of Albite Dissolution Kinetics on pH and Time at 25°C and 70°C." *Geochim. Cosmochim. Acta* 50:2481-2497.

Knauss, K. G., W. L. Bourcier, K. D. McKeegan, C. I. Merzbacher, S. N. Nguyen, F. J. Ryerson, D. K. Smith, H. C. Weed, L. Newton. 1990. "Dissolution Kinetics of a Simple Analogue Nuclear Waste Glass as a Function of pH, Time and Temperature." In *Scientific Basis for Nuclear Waste Management XIII*, eds. V. M. Oversby and P. W. Brown, Materials Research Society, Pittsburgh.

McGrail, B. P., and K. M Olson. 1992. *Evaluating Long-term Performance of In-situ Vitrified Waste Forms: Methodology and Results*. PNL-8358, Pacific Northwest Laboratory, Richland, Washington.

McGrail, B. P., and L. A. Mahoney. 1995. *Selection of a Computer Code for Hanford Low-Level Waste Engineered-System Performance Assessment*. PVTD-C95-04.01E, Pacific Northwest Laboratory, Richland, Washington.

Pigford, T. H., J. O. Blomeke, T. L. Brekke, G. A. Cowan, W. E. Falconer, N. J. Grant, J. R. Johnson, J. M. Matusek, R. R. Parizek, R. L. Pigford, D. E. White. 1983. *A Study of the Isolation System for Geologic Disposal of Radioactive Wastes*, National Academy Press, Washington, D.C.

Rustad, J. R., and B. P. Hay. 1995. "Molecular Dynamics Calculation of the Deprotonation of Orthosilicic Acid in Aqueous Solution." *Geochim. Cosmochim. Acta* **107**:433.

Wolery, T. J. 1992. *EQ3/6, A Software Package for Geochemical Modeling of Aqueous Systems: Package Overview and Installation Guide*. UCRL-MA-110662 PT I, Lawrence Livermore National Laboratory, Livermore, California.

APPENDIX A

Computation of Surface Area Change From Flow-Through Data

APPENDIX A

Computation of Surface Area Change From Flow-Through Data

Nomenclature

Variable	Description
C	concentration, g/m^3
m	mass, g
N	number of glass particles
Q	flow rate, m^3/d
r	radius of glass particle, m
S	surface area, m^2
t	time, d
Greek Symbols	
Δ	difference operator
π	pi
ρ	glass density, g/m^3
Subscripts	
i,j	time period
k	glass component, B, Si, etc.
o	reference value at time=0

The purpose of this note is to illustrate a computational procedure for computing the change in glass surface area that occurs during glass corrosion tests, such as the PCT and SPFT test. The analysis presented here is intended for use in tests where the glass has been ground and sieved to a specific mesh size. We assume here that the ground glass is adequately represented by spherically-shaped particles.

With the above assumptions, the total surface area of the glass at a time interval i, is given by:

$$S_i = 4\pi N r_i^2. \qquad \text{(A1)}$$

Equation (A1) can be written in terms of variables that are known, namely the glass density and total mass by a simple change of variables. We first need an expression for N. This can be found by realizing that

$$m_o = \frac{4}{3} N \pi \rho r_o^3. \quad (A2)$$

Solving Equation (A2) for N gives

$$N = \frac{3m_o}{4\pi\rho r_o^3}. \quad (A3)$$

Substituting Equation (A3) into A(1) gives

$$S_i = \frac{3m_o}{\rho r_o^3} r_i^2. \quad (A4)$$

The remaining unknown, r_i, can be eliminated from Equation (A4) by first writing an expression for the total mass of glass at any time i that is analogous to Equation (A2)

$$m_i = \frac{4}{3} N \pi \rho r_i^3. \quad (A5)$$

Substituting Equation (A3) into Equation (A5) gives

$$m_i = m_o \frac{r_i^3}{r_o^3}. \quad (A6)$$

Solving Equation (A6) for r_i,

$$r_i = \left(\frac{m_i}{m_o}\right)^{1/3} r_o. \quad (A7)$$

Substituting Equation (A7) into Equation (A4) we arrive at the following expression

$$S_i = \frac{3}{\rho r_o} m_o^{1/3} m_i^{2/3}. \quad (A8)$$

Equation (A8) provides an expression for the surface area at time i once m_i has been computed. For a Single-Pass Flow-Through Test, this is done with the following expression:

$$m_i = m_o - \frac{1}{f_k}\left[\sum_{j=1}^{i-1} Q_j C_{j,k} \Delta t_j + Q_i C_{i,k} \frac{\Delta t_i}{2}\right], \quad i \geq 1 \quad (A9)$$

Equation (A9) represents a time-centered approximation to the surface area at the current time step. The summation term represents the accumulated mass loss up to time step i-1 and the second term in the brackets represents 1/2 of the total mass loss from time i-1 to i. This expression is readily implemented in a spreadsheet program or other computational software.

The element concentration used in Equation (A9) for the mass loss calculation should be an element such as B, Na, or Si that is expected to be most representative of the true amount of glass dissolved in the test.

APPENDIX B

SPFT Data Summary

APPENDIX B

SPFT Test Data Summary

This appendix contains a summary of the SPFT test results on the six test glasses. Solution concentration data are given in mg/L and have not been background corrected. The temperature of a test can be found by inspecting the Test ID column. For example, tests with ID "PRIV95-90-1" were run at 90°C whereas tests with ID "PRIV95-40-1" were run at 40°C. The reader should also note that the pH 9 buffer solution used in the 90°C tests was inadvertantly made to approximately double the specified ionic strength.

Table B.1. Summary of SPFT Results for the 0.005m H_3BO_3 + 0.002m LiOH Buffer

Test ID	Glass ID	Time (d)	Flow (mL/d)	pH	Δmass	Area (m^2)	Al	B	Ca	Li	Na	Si
PRIV95-40-1	LD4-9012	4	32.41	8.66	0.02%	0.02142	-0.3	53	0.13	14.2	1.5	0.44
PRIV95-40-1	LD4-9012	7	32.28	8.99	0.04%	0.02142	0.3	53	0.15	14.3	1.3	0.6
PRIV95-40-1	LD4-9012	11	32.57	8.94	0.09%	0.02141	-0.3	52	0.08	14.1	1.1	0.82
PRIV95-40-1	LD4-9012	14	32.18	8.88	0.11%	0.02141	-0.3	50	0.06	13.2	1	0.78
PRIV95-70-1	LD4-9012	4	64.17	8.79	0.35%	0.02113	1.3	51	-0.02	13.1	3.5	3.5
PRIV95-70-1	LD4-9012	7	66.68	8.99	0.72%	0.02108	1.5	51	-0.02	13.1	3.2	4.7
PRIV95-70-1	LD4-9012	10	63.35	9.02	1.07%	0.02103	1.5	50	-0.02	12.8	2.8	4.8
PRIV95-70-1	LD4-9012	14	64.94	9.02	1.56%	0.02097	1.7	48	-0.02	12.8	2.6	4.8
PRIV95-90-1	LD4-9012	1	94.01	8.89	0.34%	0.02114	2.5	120	0.82	29	16	9.4
PRIV95-90-1	LD4-9012	3	97.56	8.93	1.30%	0.02105	2.9	120	0.64	29	9.1	12.6
PRIV95-90-1	LD4-9012	5	127.22	8.99	2.39%	0.02090	3	120	0.53	30	7.8	11
PRIV95-90-1	LD4-9012	7	97.34	8.96	3.35%	0.02076	3.4	120	0.15	30	8.4	12.7
PRIV95-90-1	LD4-9012	10	81.16	8.97	4.68%	0.02059	3.7	120	0.1	30	8.8	14
PRIV95-40-1	LD6-5412	4	32.47	8.61	0.07%	0.02066	-0.3	47	0.32	13.1	1.4	1.44
PRIV95-40-1	LD6-5412	7	32.41	8.99	0.13%	0.02065	-0.4	51	0.32	14.2	1.4	1.54
PRIV95-40-1	LD6-5412	11	32.29	8.92	0.21%	0.02064	-0.4	52	0.28	14.3	1.2	1.51
PRIV95-40-1	LD6-5412	14	32.16	8.83	0.26%	0.02063	-0.4	51	0.21	14.1	1.2	1.48
PRIV95-70-1	LD6-5412	4	65.03	8.95	0.58%	0.02042	1.6	51	0.63	13.3	4.1	5.7
PRIV95-70-1	LD6-5412	7	66.15	8.79	1.03%	0.02035	1.6	51	0.58	13.5	3.6	5.9
PRIV95-70-1	LD6-5412	10	63.10	9.02	1.45%	0.02029	1.5	53	0.6	14	3.5	5.7
PRIV95-70-1	LD6-5412	14	65.21	9.02	1.98%	0.02022	1.3	51	0.6	14.2	3.4	5.2
PRIV95-90-1	LD6-5412	1	94.38	8.89	0.48%	0.02040	3	117	1.8	30	14.7	13
PRIV95-90-1	LD6-5412	3	98.31	8.94	1.47%	0.02030	2.9	119	1.7	31	8.2	13
PRIV95-90-1	LD6-5412	5	98.31	8.98	2.31%	0.02018	2.6	109	1.5	30	7	11
PRIV95-90-1	LD6-5412	7	97.56	8.96	3.15%	0.02006	2.8	114	2.8	31	7	11
PRIV95-90-1	LD6-5412	10	99.35	8.98	4.54%	0.01991	3.1	119	2.2	31	6.8	12

Table B.1. Summary of SPFT Results for the 0.005m H_3BO_3 + 0.002m LiOH Buffer

Test ID	Glass ID	Time (d)	Flow (mL/d)	pH	Δmass	Area (m^2)	Al	B	Ca	Li	Na	Si
PRIV95-40-1	L7-15	4	32.25	8.59	0.05%	0.02171	0.3	54	0.29	14	1.1	1.07
PRIV95-40-1	L7-15	7	33.36	8.96	0.09%	0.02170	0.3	54	0.31	13.7	0.9	1.11
PRIV95-40-1	L7-15	11	31.50	8.92	0.14%	0.02169	0.34	54	0.19	13.7	0.92	1.1
PRIV95-40-1	L7-15	14	32.55	8.90	0.17%	0.02169	0.3	53	0.24	13.8	0.95	1.04
PRIV95-70-1	L7-15	4	62.28	8.81	0.50%	0.02149	1.5	53	0.59	14.4	3	5.7
PRIV95-70-1	L7-15	7	71.34	8.96	0.94%	0.02142	1.3	52	0.6	14.5	2.9	5.9
PRIV95-70-1	L7-15	10	72.67	9.01	1.35%	0.02136	1.5	52	0.52	13.6	2.3	5.3
PRIV95-70-1	L7-15	14	70.57	9.02	1.85%	0.02129	1.5	50	0.48	12.7	2	5.1
PRIV95-90-1	L7-15	1	95.73	8.82	0.44%	0.02111	2.7	120	1.7	31	9.4	12.7
PRIV95-90-1	L7-15	3	98.59	8.91	1.25%	0.02102	2.7	110	2.5	29	5.7	11.5
PRIV95-90-1	L7-15	5	99.73	8.95	2.06%	0.02090	2.4	110	1.5	30	5.2	11.4
PRIV95-90-1	L7-15	7	98.82	8.95	2.87%	0.02079	2.8	110	2.3	30	5.1	11.4
PRIV95-90-1	L7-15	10	99.95	8.95	4.13%	0.02064	2.7	120	2	31	5.2	11.8
PRIV95-40-1	L7-25	4	32.63	8.69	0.11%	0.02112	0.87	54	0.22	14.4	9.5	2.14
PRIV95-40-1	L7-25	7	32.52	9.04	0.18%	0.02111	0.77	52	0.25	14.3	7.2	1.73
PRIV95-40-1	L7-25	11	32.70	9.01	0.26%	0.02110	0.6	52	0.17	13.8	6	1.39
PRIV95-40-1	L7-25	14	32.33	8.98	0.32%	0.02109	-0.5	53	0.18	13.9	5.6	1.5
PRIV95-70-1	L7-25	4	65.59	8.85	0.67%	0.02086	2	50	0.57	12.6	14.6	6.2
PRIV95-70-1	L7-25	7	66.44	9.04	1.18%	0.02077	2	50	0.31	13	11.8	6.2
PRIV95-70-1	L7-25	10	63.42	9.10	1.65%	0.02071	2	51	0.31	13.6	10.3	5.9
PRIV95-70-1	L7-25	14	65.42	9.10	2.30%	0.02063	2.1	53	0.29	13.8	9.2	6
PRIV95-90-1	L7-25	1	95.92	9.23	0.68%	0.02048	3.8	110	1.1	28	68	16.7
PRIV95-90-1	L7-25	3	100.92	9.09	2.15%	0.02034	4.3	110	0.81	30	46	17.4
PRIV95-90-1	L7-25	5	105.45	9.10	3.67%	0.02013	4.3	120	0.76	31	35	17
PRIV95-90-1	L7-25	7	99.18	9.03	4.91%	0.01994	3.8	110	1.6	29	22	14.9
PRIV95-90-1	L7-25	10	110.08	9.01	6.96%	0.01971	3.4	120	1.8	31	17	14.7
PRIV95-40-1	SRM622	4	31.83	8.99	0.21%	0.02119	-0.06	50	1.7	14.1	2.9	5.4
PRIV95-40-1	SRM622	7	31.82	8.99	0.29%	0.02117	-0.06	50	0.9	13.7	1.6	3.1
PRIV95-40-1	SRM622	11	31.43	8.97	0.39%	0.02116	-0.06	52	0.65	14	1.1	2.6
PRIV95-40-1	SRM622	14	31.51	8.95	0.46%	0.02115	-0.06	51	0.53	13.6	0.8	2.4
PRIV95-70-1	SRM622	4	64.32	8.99	0.65%	0.02094	0.32	51	2	13.8	2.8	8.3
PRIV95-70-1	SRM622	7	64.76	8.98	1.07%	0.02086	0.3	51	1.9	14.1	2.4	7.3
PRIV95-70-1	SRM622	10	62.33	9.05	1.42%	0.02081	0.2	50	1.6	13.4	1.9	6.2
PRIV95-70-1	SRM622	14	63.80	9.07	1.92%	0.02075	-0.2	51	1.7	13.8	2.2	6.5
PRIV95-90-1	SRM622	1	92.40	8.90	0.67%	0.02088	0.41	110	5.7	30	18	24
PRIV95-90-1	SRM622	3	96.50	8.95	1.72%	0.02076	0.39	110	4.6	30	5.2	18
PRIV95-90-1	SRM622	5	93.48	9.02	2.74%	0.02062	0.41	110	4.7	31	5.2	18
PRIV95-90-1	SRM622	7	88.78	8.98	3.71%	0.02048	0.35	120	5.1	30	5.4	18
PRIV95-90-1	SRM622	10	87.28	8.97	5.22%	0.02030	0.45	120	5	31	6.1	19
PRIV95-40-1	L8-3	4	32.62	8.64	0.04%	0.02067	0.3	57	0.24	15.2	2.7	0.89
PRIV95-40-1	L8-3	7	32.55	8.97	0.08%	0.02066	-0.3	58	0.25	15.6	2.3	0.97

Table B.1. Summary of SPFT Results for the 0.005m H_3BO_3 + 0.002m LiOH Buffer

Test ID	Glass ID	Time (d)	Flow (mL/d)	pH	Δmass	Area (m^2)	Al	B	Ca	Li	Na	Si
PRIV95-40-1	L8-3	11	32.64	8.96	0.12%	0.02066	-0.3	57	0.17	15.9	1.9	0.85
PRIV95-40-1	L8-3	14	32.16	8.93	0.15%	0.02065	-0.4	54	0.17	15.7	1.8	0.81
PRIV95-70-1	L8-3	4	64.26	8.95	0.42%	0.02066	1.1	53	0.33	13.6	5.9	4.3
PRIV95-70-1	L8-3	7	66.57	8.76	0.76%	0.02061	1.2	52	0.36	13.6	4.8	4.5
PRIV95-70-1	L8-3	10	63.66	9.00	1.07%	0.02056	0.8	53	0.38	13.9	4.1	4.3
PRIV95-70-1	L8-3	14	65.52	9.01	1.47%	0.02052	0.8	53	0.34	13.7	3.7	4.1
PRIV95-90-1	L8-3	1	98.43	8.90	0.35%	0.02016	1.8	110	0.94	28	20	9.1
PRIV95-90-1	L8-3	3	101.70	8.94	1.07%	0.02009	1.7	120	0.96	30	11	9.2
PRIV95-90-1	L8-3	5	102.86	8.98	1.74%	0.02000	1.6	110	1.1	30	8.6	8.4
PRIV95-90-1	L8-3	7	101.73	8.93	2.39%	0.01991	1.8	110	1.9	28	7.6	8.2
PRIV95-90-1	L8-3	10	103.10	8.97	3.45%	0.01979	1.5	110	1.5	28	7	8.9

Table B.2. Summary of SPFT Results for the 0.005m LiCl + 0.0107m LiOH Buffer

Test ID	Glass ID	Time (d)	Flow (mL/d)	pH	Δmass	Area (m^2)	Al	B	Ca	Li	Na	Si
PRIV95-40-1	LD4-9012	4	32.99	11.75	1.04%	0.02119	5.3	2.5	0.22	107	13.3	20.4
PRIV95-40-1	LD4-9012	7	32.31	11.89	1.78%	0.02107	5.3	2.4	0.16	107	13.2	19.7
PRIV95-40-1	LD4-9012	11	32.06	11.89	2.77%	0.02094	5.2	2.4	0.09	105	12.3	19.8
PRIV95-40-1	LD4-9012	14	32.04	11.87	3.50%	0.02082	5.4	2.4	0.08	105	12.3	19.6
PRIV95-70-1	LD4-9012	4	64.77	11.88	4.07%	0.02119	10.2	4.8	-0.02	112	25	41
PRIV95-70-1	LD4-9012	7	66.81	11.83	7.38%	0.02065	10.6	5	-0.02	117	27	43
PRIV95-70-1	LD4-9012	10	64.02	11.84	10.40%	0.02019	10.1	4.7	-0.02	114	25	41
PRIV95-70-1	LD4-9012	14	66.25	11.90	14.67%	0.01965	10.3	4.8	-0.02	112	26	42
VEN95-90-1	LD4-9012	1	100.29	11.79	1.83%	0.02198	13	5.85	0.08	109	36	49
VEN95-90-1	LD4-9012	3	100.32	11.84	5.42%	0.02158	12.2	5.7	0.1	108	31	48
VEN95-90-1	LD4-9012	5	102.20	11.85	8.92%	0.02104	12.1	5.4	0.1	108	29	46
VEN95-90-1	LD4-9012	7	100.96	11.83	12.53%	0.02050	13	5.6	0.07	109	30	48
PRIV95-40-1	LD6-5412	4	32.78	11.75	0.91%	0.02063	5	1.25	1.9	109	12.1	18
PRIV95-40-1	LD6-5412	7	31.92	11.88	1.57%	0.02052	5	1.24	1.8	109	11.9	18
PRIV95-40-1	LD6-5412	11	31.85	11.89	2.47%	0.02041	4.9	1.2	1.9	111	12.3	18.3
PRIV95-40-1	LD6-5412	14	31.84	11.88	3.12%	0.02030	4.8	1.18	1.9	108	11.9	17.7
PRIV95-70-1	LD6-5412	4	64.58	11.86	2.97%	0.02051	7.1	2.4	0.66	113	19	30
PRIV95-70-1	LD6-5412	7	67.03	11.82	5.06%	0.02016	6.6	2	0.86	110	17	27
PRIV95-70-1	LD6-5412	10	63.65	11.92	7.04%	0.01988	6.8	1.8	2.4	108	17	27
PRIV95-70-1	LD6-5412	14	66.05	11.92	9.88%	0.01953	6.8	1.8	2.5	113	18	28
VEN95-90-1	LD6-5412	1	101.43	11.94	1.31%	0.02083	8.7	2.1	3.1	111	30	34
VEN95-90-1	LD6-5412	3	101.16	11.89	3.46%	0.02059	7.3	1.7	1.5	110	21	28
VEN95-90-1	LD6-5412	5	102.26	11.89	5.72%	0.02028	7.4	1.7	1.5	109	21	29
VEN95-90-1	LD6-5412	7	102.31	11.86	8.44%	0.01992	9.5	2.2	1.9	111	24	35
PRIV95-40-1	L7-15	4	33.33	11.86	0.83%	0.02131	4.8	1.19	1.3	108	8.2	17.6

Table B.2. Summary of SPFT Results for the 0.005m LiCl + 0.0107m LiOH Buffer

Test ID	Glass ID	Time (d)	Flow (mL/d)	pH	Δmass	Area (m^2)	Al	B	Ca	Li	Na	Si
PRIV95-40-1	L7-15	7	32.52	11.75	1.47%	0.02120	4.6	1.23	1.38	105	8.1	18.6
PRIV95-40-1	L7-15	11	32.31	11.90	2.28%	0.02110	4.3	1.16	1.3	106	8.1	17.6
PRIV95-40-1	L7-15	14	32.50	11.90	2.92%	0.02100	4.8	1.22	1.3	109	8.6	18.5
PRIV95-70-1	L7-15	4	64.82	11.88	2.76%	0.02109	7.2	2.1	1.8	112	14	30
PRIV95-70-1	L7-15	7	68.08	11.83	4.94%	0.02074	7	2	1.7	109	14	30
PRIV95-70-1	L7-15	10	65.14	11.89	7.16%	0.02042	7.5	2.1	1.8	109	15	32
PRIV95-70-1	L7-15	14	67.24	11.92	9.93%	0.02006	7	1.8	1.7	105	13	29
GDL-95L-90-1	L7-15	1	102.43	11.74	1.44%	0.02139	9.6	2.5	2.43	113	23	40
GDL-95L-90-1	L7-15	3	100.72	11.86	3.99%	0.02110	8.6	2.25	2.13	113	19	36
GDL-95L-90-1	L7-15	5	100.25	11.93	6.32%	0.02075	7.6	2.1	1.9	113	17	33
GDL-95L-90-1	L7-15	7	99.72	11.74	8.64%	0.02041	7.6	2.05	1.85	111	17	33
GDL-95L-90-1	L7-15	10	97.91	11.78	12.05%	0.01998	7.7	2.14	1.75	113	18	33
PRIV95-40-1	L7-25	4	34.34	11.59	1.36%	0.02095	6.4	1.65	0.91	106	20.4	24.1
PRIV95-40-1	L7-25	7	33.08	11.88	2.31%	0.02079	6	1.6	0.92	103	19.7	23.4
PRIV95-40-1	L7-25	11	32.72	11.89	3.63%	0.02063	6.3	1.6	0.94	104	20.8	24.4
PRIV95-40-1	L7-25	14	32.9	11.91	4.62%	0.02046	6.9	1.6	0.9	106	22.2	24.6
PRIV95-70-1	L7-25	4	65.13	11.89	4.46%	0.02089	10.9	2.8	0.7	115	45	42
PRIV95-70-1	L7-25	7	61.79	11.88	7.41%	0.02036	9.7	2.6	0.64	110	41	39
PRIV95-70-1	L7-25	10	66.56	11.85	10.51%	0.01992	9.6	2.5	0.58	112	39	38
PRIV95-70-1	L7-25	14	67.93	11.94	15.05%	0.01936	10.7	2.8	0.7	107	40	41
GDL-95L-90-1	L7-25	1	101.65	11.93	2.39%	0.02077	15	3.7	0.34	107	125	57
GDL-95L-90-1	L7-25	3	100.55	11.92	6.63%	0.02030	13.1	3.35	0.42	103	96	51
GDL-95L-90-1	L7-25	5	101.20	11.95	10.89%	0.01969	12.9	3.36	0.45	110	76	51
GDL-95L-90-1	L7-25	7	100.03	11.69	15.27%	0.01907	13.9	3.55	0.38	116	66	53
GDL-95L-90-1	L7-25	10	99.51	11.86	21.81%	0.01826	13.7	3.49	0.32	114	54	53
PRIV95-40-1	SRM622	4	33.24	11.70	0.97%	0.02071	0.6		0.46	110	8.8	24
PRIV95-40-1	SRM622	7	32.50	11.91	1.66%	0.02059	0.6		0.42	110	8.5	23
PRIV95-40-1	SRM622	11	32.18	11.88	2.56%	0.02048	0.5		5.6	114	9.3	23
PRIV95-40-1	SRM622	14	32.42	11.89	3.24%	0.02037	1		4.9	117	9.2	23
PRIV95-70-1	SRM622	4	65.92	11.85	5.52%	0.02078	0.8	0.31	2.6	113	32	70
PRIV95-70-1	SRM622	7	67.65	11.82	9.72%	0.02008	0.8	0.21	2.4	110	30	69
PRIV95-70-1	SRM622	10	64.72	11.89	13.43%	0.01950	0.8	0.05	2.3	107	28	64
PRIV95-70-1	SRM622	14	66.84	11.91	17.76%	0.01891	0.7	0.04	2.1	109	25	54
VEN95-90-1	SRM622	1	98.86	11.91	2.39%	0.02132	0.7	0.06	3.5	111	39	82
VEN95-90-1	SRM622	3	98.35	11.76	8.36%	0.02072	0.7	0.04	2.2	109	48	103
VEN95-90-1	SRM622	5	99.99	11.81	14.02%	0.01986	0.6	0.03	1.9	108	45	96
VEN95-90-1	SRM622	7	100.52	11.83	19.24%	0.01904	0.6	-0.03	1.7	108	41	88
PRIV95-40-1	L8-3	4	30.85	11.72	0.46%	0.02058	2.1	0.15	0.27	110	7.3	9.8
PRIV95-40-1	L8-3	7	29.90	11.92	0.83%	0.02053	2.5	0.15	0.28	110	8.2	11
PRIV95-40-1	L8-3	11	29.62	11.89	1.34%	0.02046	2.6	-0.1	0.26	110	8.4	11.3
PRIV95-40-1	L8-3	14	29.81	11.92	1.69%	0.02041	2.4	-0.01	0.24	110	7.5	10.2

Table B.2. Summary of SPFT Results for the 0.005m LiCl + 0.0107m LiOH Buffer

Test ID	Glass ID	Time (d)	Flow (mL/d)	pH	Δmass	Area (m^2)	Al	B	Ca	Li	Na	Si
PRIV95-70-1	L8-3	4	61.21	11.87	2.41%	0.02045	5.2	0.76	-0.01	112	21	26
PRIV95-70-1	L8-3	7	62.80	11.76	4.34%	0.02015	5.2	0.8	0.03	110	20	27
PRIV95-70-1	L8-3	10	59.94	11.89	6.04%	0.01989	5.2	0.63	-0.01	111	20	25
PRIV95-70-1	L8-3	14	62.04	11.94	8.30%	0.01961	5	0.57	-0.01	111	19	24
GDL-95L-90-1	L8-3	1	100.47	11.86	1.42%	0.02031	7.7	1.4	0.18	117	45	37
GDL-95L-90-1	L8-3	3	100.43	11.89	4.65%	0.02000	8.2	1.6	0.18	120	35	42
GDL-95L-90-1	L8-3	5	101.06	11.89	7.75%	0.01956	7.8	1.5	0.2	119	31	40
GDL-95L-90-1	L8-3	7	99.94	12.01	10.58%	0.01914	7.7	1.4	0.18	117	32	37
GDL-95L-90-1	L8-3	10	97.79	11.85	14.73%	0.01865	7.5	1.4	0.16	107	31	37

APPENDIX C

Brief Description of IPAI Code

APPENDIX C

Brief Description of IPAI Code

Nomenclature

Variable	Description
c	concentration, g/m^3
E_a	activation energy, kcal/mol
K	pseudoequilibrium constant
k_o	intrinsic rate constant, mol/m^2·d
Q	ion activity product
R	gas constant, kcal/mol
S	surface area, m^2
t	time, d
T	temperature, K
V	solution mass, kg
Greek Symbols	
ξ	reaction progress, mol/kg
η	power law coefficient
σ	overall stoichiometric number for the activated complex
Subscripts	
j	chemical species

The Interactive Performance Analysis Integrator (IPAI) is a computer code for modeling the dissolution kinetics of glasses in closed-system, isothermal, laboratory tests. The current version of the code solves the rate equation

$$\frac{d\xi}{dt} = \frac{S(\xi)}{V} k_o 10^{\eta[\mathrm{pH}(\xi)]} e^{\frac{E_a}{RT}} \left[1 - \left(\frac{Q(\xi)}{K}\right)^{1/\sigma}\right]. \qquad \text{(C1)}$$

The variables pH, Q, and the concentrations of each component (c_j) are computed as a function of reaction progress (ξ) using a version of the EQ3/6 code that has been modified to output these data into formatted files that are read by the IPAI code. Glass surface area is computed with respect to ξ as described in Appendix A. Equation (C1) is integrated using a 5th-

order Runge-Kutta algorithm with adaptive time-stepping. Once $\xi(t)$ has been computed, the solution pH, Eh, and concentrations of all the glass components are computed as a function of time by linear interpolation.

IPAI runs under the Microsoft Windows™ operating system. It has capabilities for displaying simple graphs of the raw input data from EQ3/6 and the computed solution concentrations as a function of time. These same data may also be viewed in a tabular grid and the results copied to the Windows Clipboard for export into other programs, such as Microsoft Excel™.

PNL-10746
UC-510

DISTRIBUTION

No. of Copies

OFFSITE

2 U.S. Department of Energy
Office of Scientific and
Technical Information

William L. Bourcier
Lawrence Livermore National Lab
7000 East Avenue
Mail Stop L-219
Livermore, CA 94550

William L. Ebert
Argonne National Laboratory
Building 205
9700 South Cass Avenue
Argonne, IL 60439-4837

David K. Peeler
Westinghouse Savannah River
Company
106 Common Court
Aiken, SC 29803

Denis M. Strachan
Argonne National Laboratory
Building 205
9700 South Cass Avenue
Argonne, IL 60439-4837

No. of Copies

ONSITE

4 **U.S. Department of Energy**
Richland Operations Office
N. R. Brown, S7-54
Public Reading Room, H2-53
RL Docket File, H5-36 (2)

3 **Westinghouse Hanford Company**
C. R. Eiholzer, H0-36
F. M. Mann, H0-36
G. F. Williamson, G6-13

15 **Pacific Northwest Laboratory**
X. Feng, P8-44
J. H. Holbrook, K9-81
P. R. Hrma, P8-37
B. P. McGrail, K2-44 (5)
W. G. Richmond, K6-51
J. H. Westsik, Jr., K9-80
Publishing Coordination
Technical Report Files, K1-11 (5)